ESAIM: M2AN 57 (2023) 1195–1223
https://doi.org/10.1051/m2an/2023001

ESAIM: Mathematical Modelling and Numerical Analysis
www.esaim-m2an.org

ANALYSIS OF A METHOD TO COMPUTE MIXED-MODE STRESS INTENSITY FACTORS FOR NON-PLANAR CRACKS IN THREE-DIMENSIONS

Benjamin E. Grossman-Ponemon[1,2], Matteo Negri[3] and Adrian J. Lew[1,*]

Abstract. In this work, we present and prove results underlying a method which uses functionals derived from the interaction integral to approximate the stress intensity factors along a three-dimensional crack front. We first prove that the functionals possess a pair of important properties. The functionals are well-defined and continuous for square-integrable tensor fields, such as the gradient of a finite element solution. Furthermore, the stress intensity factors are representatives of such functionals in a space of functions over the crack front. Our second result is an error estimate for the numerical stress intensity factors computed *via* our method. The latter property of the functionals provides a recipe for numerical stress intensity factors; we apply the functionals to the gradient of a finite element approximation for a specific set of crack front variations, and we calculate the stress intensity factors by inverting the mass matrix for those variations.

Mathematics Subject Classification. 46N40, 70G75, 74G15, 74R10.

Received April 22, 2022. Accepted December 28, 2022.

1. Introduction

The stress intensity factors, which characterize the stress singularities near the front of a three-dimensional crack, are important parameters for predicting the failure of engineering structures. In [17], a method to compute the stress intensity factors along the front of a three-dimensional crack was introduced; in this paper, we prove convergence and error estimates for such method.

In the literature, there are a variety of approaches to compute the stress intensity factors, which generally fall into one of two categories. The first category includes extrapolation-based methods. These methods sample the stress or displacement field around the crack and fit known asymptotic behavior (*cf.* [35]). The stress intensity factors are estimated from the fitting parameters [7, 33]. In the second category are methods where the stress intensity factors (or combinations thereof) are the outputs of certain functionals applied to the displacement field or its gradient. Among these are methods based on the J-integral [8,28] such as the J_k-integrals [19,27], the Contour Integral and Cutoff Function Methods [4,31,32] and the Quasi-Dual Function Method [12,35], and the interaction integral [34]. Most of these approaches originated in the study of two-dimensional crack problems,

---

Keywords and phrases. Fracture mechanics, singularities, stress intensity factors.

[1] Department of Mechanical Engineering, Stanford University, Stanford, CA 94035, USA.

[2] School of Engineering, Brown University, Providence, RI 02912, USA.

[3] Department of Mathematics, University of Pavia, Via A. Ferrata 1, 27100 Pavia, Italy.

*Corresponding author: lewa@stanford.edu

but have since been extended to three-dimensional cracks (*e.g.*, [16] shows an approach based on the interaction integral for three-dimensional cracks).

The method in [17] is based on the solution of a variational problem involving a set of three functionals $\{F_\alpha\}_\alpha$, which are derived from the interaction integral [34] and particularized for the elasticity problem of interest in the continuous setting. These functionals act on a virtual (normal) extension of the crack front v and a square-integrable tensor field. They have two important properties. First, when the tensor field is the gradient of the exact solution of the elasticity problem $\nabla \boldsymbol{u}$, they output precisely integrals of the stress intensity factors $\{K_\alpha\}_\alpha$ along the crack front $\mathcal{F}$ weighted by the virtual extension v:

$$F_\alpha[v, \nabla \boldsymbol{u}] = \int_{\mathcal{F}} v K_\alpha \,\mathrm{d}s, \quad \alpha = \mathrm{I}, \mathrm{II}, \mathrm{III}. \tag{1.1}$$

The functionals (and the interaction integral) provide an integral representation of the stress intensity factors in terms of the solution $\boldsymbol{u}$, which make them particularly suitable for numerical evaluation. Second, the functionals are continuous and affine with respect to their arguments.

Two discretizations are needed for the method. First, we consider a fixed virtual extension v of the crack front, and introduce a numerical approximation of the exact displacement gradient with a discretization length scale h_B, termed $\nabla \boldsymbol{u}^{h_B}$. In this paper and in the implementation [17], the approximate gradient is computed using the Finite Element Method (FEM, *e.g.*, that of [18]) on meshes of the problem domain with mesh size h_B. Other methods, such as the Extended Finite Element Method (XFEM [26]) or Mapped Finite Element Method (MFEM [10]), may be used instead. For a fixed virtual extension of the crack front v, convergence of the numerical gradient in the L^2-norm guarantees the convergence of the values of the functionals solely due to continuity. Second, we introduce a discretization of the virtual extensions of the crack front. In this case, we restrict ourselves to a finite dimensional subset with length scale h_F. For example, we may use piece-wise linear Lagrange finite elements over the crack front with mesh size h_F. Alternatively, we can build a spectral basis up to maximum order k_F (where k_F is treated like h_F^{-1}). By restricting the numerical stress intensity factors $\{K_\alpha^h\}_\alpha$ to the same space of the virtual displacements and endowing such space with the L^2-scalar product over the crack front, *i.e.*, the right-hand-side in (1.1), each K_α^h follows as the Riesz representative of the functional $F_\alpha[\cdot, \nabla \boldsymbol{u}^{h_B}]$ in that space. This enables the computation of approximate stress intensity factors by solving a variational problem.

Further, for each numerical stress intensity factor K_α^h we prove an error estimate of the form

$$\left\| K_\alpha - K_\alpha^h \right\|_{0,\mathcal{F}} \leq C_1 h_F^n + C_2 h_B^m h_F^{-1} \tag{1.2}$$

for constants C_1 and C_2 independent of h_B and h_F. The first term emerges from an interpolation error, and the second one from a consistency error. Success of the method hinges on these two errors converging to zero as h_B and h_F do. What complicates this effort is that the consistency error grows with decreasing h_F. For low-order finite elements and scaling the discretizations like $h_F \sim h_B$, this estimate does not guarantee that the method converges. This is the case, for example, when using the restrictions of the shape functions in the three-dimensional volumetric (or bulk) mesh to the crack front as the basis for the space of virtual extensions of the crack. In [17], such scaling between bulk and crack front meshes resulted in reduced rates of convergence of K_α^h in the L^2-norm. Convergence is guaranteed by shrinking h_B^m more quickly than h_F, where m is the order of the approximation $\nabla \boldsymbol{u}^{h_B}$ (for FEM, $m = 1/2$). Because the meshes used in the bulk and along the front are different, we term our approach the Multiple Mesh Interaction Integral method (MMII).

In this work, we prove two properties of each functional F_α, namely continuity and (1.1), and we prove the error estimate (1.2). A critical ingredient for the proof of (1.1) is to show that any smooth part (H^1) of the displacement gradient belongs to the kernel of the interaction integral. To the authors' knowledge, such a result for the interaction integral in three dimensions is novel, though a sketch proof was provided for a similar result in two dimensions in [9]. We then make use of the two properties of the functionals to derive (1.2), which stems from the variational formulation.

This paper is organized as follows. In Section 2, we introduce some preliminary definitions of the geometry in the vicinity of the crack front. We present the linear elasticity problem of interest, and state a key assumption about the decomposition of the solution into a smooth part and a part containing the familiar $r^{1/2}$ asymptotic behavior of Linear Elastic Fracture Mechanics (LEFM). In Section 3, we recapitulate the functionals and problem to define the approximate stress intensity factors, and we state as theorems the main results of the paper. Section 4 is devoted to proving the theorems, though ancillary and more technical results are relegated to the appendices. We finish with a numerical study of the convergence of the interaction integral in Section 5. Here, we address two key points. First, in computer implementations of the MMII, the functionals $\{F_\alpha\}_\alpha$ are approximated through numerical quadrature. The integrands of the functionals contain radial singularities like $r^{-1/2}$, and, depending on the choice of function space over the crack front, may also have discontinuities. These issues affect the convergence rates of standard quadrature rules under refinement of the bulk mesh, and we assess whether these errors interfere with the analytically-derived error estimate (1.2). Second, classical analysis of continuous linear functionals applied to finite element solutions (*e.g.*, [3,4]) utilizes a duality argument to prove superconvergence (often double that of the finite element error). We recapitulate these arguments in detail, and we explain where analytical shortcomings may arise in their application to our present work.

Throughout this paper, we will make use of constants C (or $C_1, C_2, \ldots$ if we wish to differentiate constants) whose value may change from line to line. We will also refer to the Sobolev space $W^{m,p}(\Omega)$, the space of functions over the domain Ω with weak derivatives up to order m in $L^p(\Omega)$, as well as the Hilbert space $H^m(\Omega) := W^{m,2}(\Omega)$. We denote the norms for these spaces with $\|\cdot\|_{m,p,\Omega}$ and $\|\cdot\|_{m,\Omega} := \|\cdot\|_{m,2,\Omega}$, respectively. For the space $H^m(\Omega)$, we will also make use of the inner product $(\cdot,\cdot)_{m,\Omega}$. When functions are vector- or tensor-valued, we will specify the range when writing the function space, *e.g.*, $W^{m,p}(\Omega;\mathbb{R}^3)$ or $W^{m,p}(\Omega;\mathbb{R}^{3\times 3})$, though we omit the range when writing the norm or inner product. For a function f of a scalar variable x, we denote the derivative by $f'(x)$, $f_{,x}$, or $\mathrm{d}f/\mathrm{d}x$. For a function $f(\xi_1,\xi_2)$, we write $f_{,1}$ or $\partial f/\partial \xi_1$ to denote the partial derivative with respect to ξ_1. Lastly, we may express points $\boldsymbol{x} \in \Omega \subset \mathbb{R}^3$ in terms of their Cartesian coordinates: $\boldsymbol{x} = x_1\boldsymbol{e}_1 + x_2\boldsymbol{e}_2 + x_3\boldsymbol{e}_3$, where $\{\boldsymbol{e}_1, \boldsymbol{e}_2, \boldsymbol{e}_3\}$ is an orthonormal basis.

2. Preliminaries

In this section, we describe the geometry in the vicinity of a three-dimensional crack front, see Fig. 1. We then state the linear elasticity problem in a cracked domain. At this point, we make a key assumption about the elasticity problem – that the displacement field near the crack front may be expressed as a sum of a tip part containing the LEFM $r^{1/2}$ asymptotes and a smooth part [11,35]. We further assume that the tip part may be decomposed into the three stress intensity modes [22,37].

2.1. Near-front coordinates

A bounded domain $\Omega \subset \mathbb{R}^3$ with Lipschitz boundary contains a sharp crack $\mathcal{C} \subset \Omega$. We assume the crack is an orientable smooth manifold with boundary[1]. We select an orientation with unit normal $\boldsymbol{N}$, and let $\mathcal{C}^\pm$ denote the crack faces where $\boldsymbol{N}$ points toward $\mathcal{C}^+$. We denote the crack front by $\mathcal{F} = \partial\mathcal{C}$, which we assume is a closed, simple, regular, smooth curve. We assume $\mathrm{dist}(\mathcal{F}, \partial\Omega) > 0$ to avoid cases where the crack front intersects the surface, such as a through crack.

Let $S = \mathrm{len}(\mathcal{F})$ be the length of the crack front, and let $\boldsymbol{F}_f : [0,S] \to \mathbb{R}^3$ be the arc length parameterization of $\mathcal{F}$ from an arbitrary starting point. If $\boldsymbol{T} : [0,S] \to \mathbb{R}^3$ is the unit tangent vector to $\mathcal{F}$ and $\boldsymbol{N} : \mathcal{C} \to \mathbb{R}^3$ is the unit normal field over $\mathcal{C}$, then for any $s \in [0,S]$, we introduce the orthonormal basis

$$\boldsymbol{g}_3(s) = \boldsymbol{T}(s) \tag{2.1}$$

$$\boldsymbol{g}_2(s) = \boldsymbol{N}(\boldsymbol{F}_f(s)) \tag{2.2}$$

$$\boldsymbol{g}_1(s) = \boldsymbol{g}_2(s) \times \boldsymbol{g}_3(s). \tag{2.3}$$

[1] Manifolds with lesser regularity may also be considered; at a minimum, we believe it necessary for the crack to be C^2 in a ρ-neighborhood of the manifold boundary.

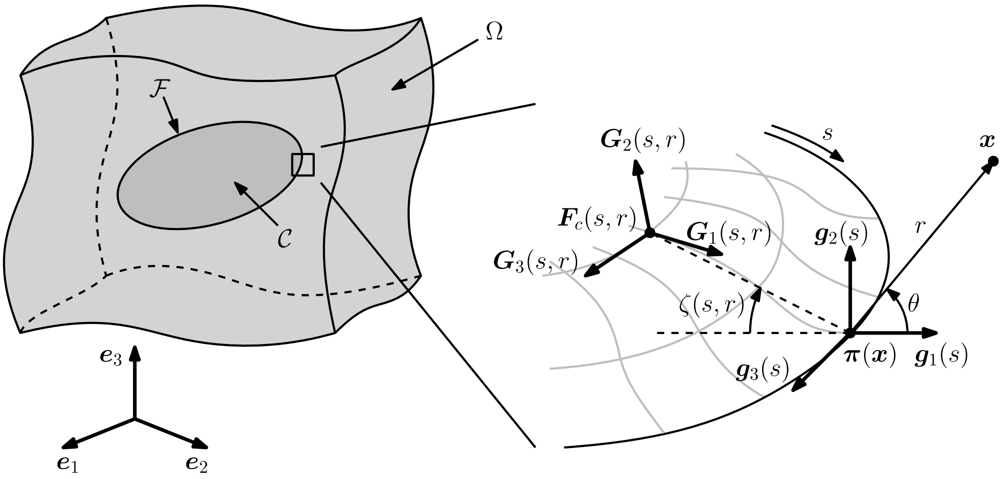

FIGURE 1. *Left*: three-dimensional domain Ω containing an internal crack $\mathcal{C}$ with crack front $\mathcal{F}$. *Right*: local description of the crack surface near the crack front. Points near the crack front may be described using coordinates (s, r, θ) along with the crack front basis $\{\boldsymbol{g}_i\}$. The crack surface is parameterized *via* the function $\boldsymbol{F}_c$, from which we define the crack surface basis $\{\boldsymbol{G}_i\}$. The inclination angle ζ is used to specify limits of θ. This figure has been reproduced from [17].

We assume that $\boldsymbol{T}$ and $\boldsymbol{N}$ are oriented such that $\boldsymbol{g}_1(s)$ is an outward-pointing vector which is tangent to $\mathcal{C}$ at $\boldsymbol{F}_f(s)$[2].

Let $\mathcal{N}_\rho$ denote the open ρ-neighborhood of $\mathcal{F}$, with $\rho > 0$ chosen small enough that the closest point projection $\boldsymbol{\pi}$ onto $\mathcal{F}$ is unique. We next characterize the near-front crack surface $\mathcal{C}_\rho = \mathcal{C} \cap \mathcal{N}_\rho$. We assume the existence of a smooth map $\boldsymbol{F}_c : [0, S] \times [0, \rho] \to \overline{\mathcal{C}_\rho}$, injective in $[0, S) \times [0, \rho]$, and with all derivatives matching at $s = 0$ and $s = S$[3]. The map is defined so that

$$\operatorname{dist}(\boldsymbol{F}_c(s, r), \mathcal{F}) = r, \qquad \boldsymbol{\pi}(\boldsymbol{F}_c(s, r)) = \boldsymbol{F}_c(s, 0) = \boldsymbol{F}_f(s). \tag{2.4}$$

Given the map $\boldsymbol{F}_c$, we introduce the angle $\zeta : [0, S] \times (0, \rho)$ as

$$\zeta(s, r) = \operatorname{atan2}((\boldsymbol{F}_c(s, r) - \boldsymbol{F}_f(s)) \cdot \boldsymbol{g}_2(s), -(\boldsymbol{F}_c(s, r) - \boldsymbol{F}_f(s)) \cdot \boldsymbol{g}_1(s)), \tag{2.5}$$

where atan2 is the two-argument inverse tangent function, taken over the principal branch $(-\pi, \pi]$. The purpose of ζ is as follows. We introduce a map from the simple region

$$\Theta = \left\{(s, r, \theta) \in \mathbb{R}^3 \,:\, s \in [0, S],\, r \in (0, \rho),\, \theta + \zeta(s, r) \in (-\pi, \pi)\right\}, \tag{2.6}$$

to the cut neighborhood $\mathcal{N}_\rho^{\mathcal{C}} = \mathcal{N}_\rho \setminus \mathcal{C}$,

$$\boldsymbol{X}(s, r, \theta) = \boldsymbol{F}_f(s) + r\cos\theta \boldsymbol{g}_1(s) + r\sin\theta \boldsymbol{g}_2(s). \tag{2.7}$$

By the regularity of the closest point projection and the distance function in $\mathcal{N}_\rho \setminus \mathcal{F}$ ([21], Thms. 4.4.10 and 4.4.11), $\boldsymbol{X}$ is a diffeomorphism.

The map $\boldsymbol{X}$ defines a set of tubular coordinates on $\mathcal{N}_\rho^{\mathcal{C}}$. Throughout this manuscript, we will abuse notation, interchanging functions whose arguments are position in space $f : \mathcal{N}_\rho^{\mathcal{C}} \to \mathbb{R}$ and coordinates $f_\Theta : \Theta \to \mathbb{R}$ (with

[2]More precisely, there exists no C^1 curve $\boldsymbol{x} : [0, \epsilon] \to \mathcal{C}$ with $\boldsymbol{x}(0) = \boldsymbol{F}_f(s)$ and $\boldsymbol{x}'(0) = \boldsymbol{g}_1(s)$, see Chapter I of [20].

[3]The function $\boldsymbol{F}_c$ is related to the notion of a collar neighborhood of $\mathcal{F}$ in $\mathcal{C}$, see Chapter I of [20].

$f_\Theta = f \circ \boldsymbol{X}$) by writing $f(s,r,\theta)$ in place of $f(\boldsymbol{x})$ and *vice versa*. Similarly, we will also interchange functions over the crack front $f : \mathcal{F} \to \mathbb{R}$ and over the arc length $f_{[0,S]} : [0,S] \to \mathbb{R}$ with $f_{[0,S]} = f \circ \boldsymbol{F}_f$. When going to coordinates, we make use of the Jacobian of $\boldsymbol{X}$ (see Appendix A)

$$rh(s,r,\theta), \tag{2.8}$$

where h denotes the stretch factor in the $\boldsymbol{g}_3$-direction

$$h(s,r,\theta) := 1 - r(\cos\theta \boldsymbol{g}_1(s) + \sin\theta \boldsymbol{g}_2(s)) \cdot \boldsymbol{T}_{,s}(s). \tag{2.9}$$

2.2. Elasticity problem

Assuming linear elasticity theory [5], we seek the displacement field $\boldsymbol{u}$ throughout the cracked body $\Omega^{\mathcal{C}} = \Omega \backslash \overline{\mathcal{C}}$ which satisfies equilibrium. In particular, the body is subjected to body force $\overline{\boldsymbol{b}}$ in the interior of the domain, tractions $\overline{\boldsymbol{t}}$ on the Neumann boundary $\partial_t \Omega^{\mathcal{C}}$, and prescribed displacements $\overline{\boldsymbol{u}}$ on the Dirichlet boundary $\partial_u \Omega^{\mathcal{C}}$. We assume $\partial_t \Omega^{\mathcal{C}} \cup \partial_u \Omega^{\mathcal{C}} = \partial \Omega^{\mathcal{C}}$, $\partial_t \Omega^{\mathcal{C}} \cap \partial_u \Omega^{\mathcal{C}} = \emptyset$, and $\mathcal{C}^{\pm} \subseteq \partial_t \Omega^{\mathcal{C}}$ (*i.e.*, we do not prescribe displacements on the crack faces). We relate the Cauchy stress tensor $\boldsymbol{\sigma}$ to the displacement gradient $\boldsymbol{\beta} = \nabla \boldsymbol{u}$ *via* the isotropic constitutive relation:

$$\sigma_{ij}(\boldsymbol{\beta}) = \mathbb{C}_{ijkl}\beta_{kl} = \lambda \beta_{kk}\delta_{ij} + \mu(\beta_{ij} + \beta_{ji}),$$

where λ and μ are the Lamé parameters (though we will also refer to Young's modulus E and Poisson's ratio ν). Here and throughout this manuscript, we make use of Einstein summation convention for repeated Roman indices. We now state the primal elasticity problem.

Problem 2.1 (Primal elasticity problem)**.** Let $\overline{\boldsymbol{b}} \in L^2(\Omega^{\mathcal{C}}; \mathbb{R}^3)$, $\overline{\boldsymbol{t}} \in H^{1/2}(\partial_t \Omega^{\mathcal{C}}; \mathbb{R}^3)$, and $\overline{\boldsymbol{u}} \in H^{3/2}(\partial_u \Omega^{\mathcal{C}}; \mathbb{R}^3)$. We seek a displacement field $\boldsymbol{u} \in H^1(\Omega^{\mathcal{C}}; \mathbb{R}^3)$ which solves

$$\begin{aligned} -\mathrm{div}(\boldsymbol{\sigma}(\nabla \boldsymbol{u})) &= \overline{\boldsymbol{b}} && \text{in } \Omega^{\mathcal{C}}, \\ \boldsymbol{\sigma}(\nabla \boldsymbol{u}) \cdot \boldsymbol{n} &= \overline{\boldsymbol{t}} && \text{on } \partial_t \Omega^{\mathcal{C}}, \\ \boldsymbol{u} &= \overline{\boldsymbol{u}} && \text{on } \partial_u \Omega^{\mathcal{C}}. \end{aligned} \tag{2.10}$$

We make the following assumption regarding the solution to Problem 2.1.

Assumption 2.2 (Near-front decomposition of the elasticity solution)**.** *We assume that the solution to Problem 2.1 may be decomposed as*

$$\boldsymbol{u}(\boldsymbol{x}) = \boldsymbol{u}_S(\boldsymbol{x}) + \sum_{\alpha=\mathrm{I}}^{\mathrm{III}} K_\alpha(s) r^{1/2} \psi_i^\alpha(\theta) \boldsymbol{g}_i(s), \tag{2.11}$$

for any $\boldsymbol{x} \in \mathcal{N}_\rho^{\mathcal{C}}$ with tubular coordinates (s,r,θ). The function $\boldsymbol{u}_S \in H^2(\Omega^{\mathcal{C}}; \mathbb{R}^3)$, while $\{K_\alpha\}_\alpha \subset H^2(\mathcal{F})$ are termed the stress intensity factors *of $\boldsymbol{u}$ for modes $\alpha = \mathrm{I}, \mathrm{II}, \mathrm{III}$. The functions $\{\psi_i^\alpha\}_{\alpha,i} \subset C^\infty(\mathbb{R})$ (provided in Appendix B of [17]) are of the form $C_1 \cos\left(\frac{\theta}{2}\right) + C_2 \cos\left(\frac{3\theta}{2}\right)$ or $C_1 \sin\left(\frac{\theta}{2}\right) + C_2 \sin\left(\frac{3\theta}{2}\right)$, where the constants depend only on the elastic moduli.*

In general, it is not known if the decomposition (2.11) always holds under the regularity assumptions of Problem 2.1. One result comes from Costabel *et al.* [11], in which the authors prove that, for an infinite domain $\Omega = \mathbb{R}^3$ containing a smooth crack with closed, smooth front, and with body force $\overline{\boldsymbol{b}} \in C^\infty(\mathbb{R}^3; \mathbb{R}^3)$, as $r \to 0$ the solution has the decomposition

$$\boldsymbol{u}(\boldsymbol{x}) = \sum_{k=0}^{K} \sum_{j=1}^{N(k)} c_j^k(s) r^{1/2+k} \boldsymbol{\psi}_j^k(s,\theta) + \boldsymbol{u}_{S,K}(\boldsymbol{x}) \tag{2.12}$$

for any integer $K \geq 0$. The functions $c_j^k(s)$ belong to $C^\infty(\mathcal{F})$, while the vector-valued functions $\boldsymbol{\psi}_j^k(s,\theta)$ depend only on the linear operator and the type of boundary conditions prescribed on the crack faces. The smooth part $\boldsymbol{u}_{S,K}$ belongs to $H^{K+1}(\Omega;\mathbb{R}^3)$.

We note the s-dependency in the vector functions $\boldsymbol{\psi}_j^k(s,\theta)$ in (2.12), which we have not assumed in (2.11). Instead, we have followed the common assumption in the literature for asymptotic expansions around a crack front that $\boldsymbol{\psi}_j^k(s,\theta) = \psi_{jl}^k(\theta)\boldsymbol{g}_l(s)$. For example, Leblond and Torlai [22] assumed a similar decomposition for the stress field when analyzing the leading-order stresses near an arbitrary three-dimensional crack. Meanwhile, Yosibash *et al.* [36] computed an asymptotic expansion for the displacement field near cracks with a circular crack front of radius R. Yosibash *et al.* assumed an asymptotic expansion of the form (*cf.* [36], Eq. (64))

$$\boldsymbol{u}(\boldsymbol{x}) = \sum_{l=0}^{\infty}\sum_{k=0}^{\infty} \frac{\mathrm{d}^l A_k(s)}{\mathrm{d}s^l} r^{\alpha_k} \sum_{j=0}^{\infty}\left(\frac{r}{R}\right)^j \sum_{i=1}^{3} \psi_{ijkl}(\theta)\boldsymbol{g}_i(s). \tag{2.13}$$

For a penny-shaped crack with arbitrary loading ([36], Eq. (94)), the lowest-order displacement terms in the asymptotic expansion coincide precisely with (2.11). Lastly, in [12], Costabel *et al.* derive the asymptotic structure for an infinite straight edge. Here, the eigenfunctions for the leading-order terms do not possess s-dependency.

Without a result that explicitly states the dependence of $\{\psi_i^\alpha\}_i$ on θ, the definition of the stress intensity factors needs to be revised. Assumption 2.2 allows us to proceed. Of course, our results apply for displacements $\boldsymbol{u}$ of the form (2.11).

The form of $\boldsymbol{u}$ in (2.11) and (2.12) corresponds to the eigenfunction expansion in the vicinity of a three-dimensional edge, which we briefly summarize here. A more complete treatment may be found in Yosibash [35]. The functions $\{\psi_i^\alpha\}_{\alpha,i}$ are determined from the following problem around the crack front.

Problem 2.3. Let $\Omega = \mathbb{R}^3$, $\mathcal{C} = \{\boldsymbol{x} \in \mathbb{R}^3 \,:\, x_1 \leq 0,\, x_2 = 0\}$ and $\mathcal{F} = \{\boldsymbol{x} \in \mathbb{R}^3 \,:\, x_1 = x_2 = 0\}$. For such geometry, the tubular coordinates are given by the usual cylindrical coordinates. For each mode $\alpha = \mathrm{I}, \mathrm{II}, \mathrm{III}$, $\boldsymbol{w}(\boldsymbol{x}) = r^{1/2}\psi_i^\alpha(\theta)\boldsymbol{e}_i$ solves

$$\begin{aligned} -\mathrm{div}(\boldsymbol{\sigma}(\nabla\boldsymbol{w})) &= \boldsymbol{0} \qquad \text{in } \Omega\setminus\mathcal{C},\\ \boldsymbol{\sigma}(\nabla\boldsymbol{w})\cdot \mp\boldsymbol{e}_2 &= \boldsymbol{0} \qquad \text{on } \mathcal{C}^\pm \end{aligned} \tag{2.14}$$

along with the following conditions:

(1) for $\alpha = \mathrm{I}$, $\psi_3^{\mathrm{I}} \equiv 0$, while ψ_1^{I} and ψ_2^{I} are even in θ, and $\lim_{r\to 0}\sqrt{2\pi r}\;\sigma_{22}(\nabla\boldsymbol{w}(r,0)) = 1$;
(2) for $\alpha = \mathrm{II}$, $\psi_3^{\mathrm{II}} \equiv 0$, while ψ_1^{II} and ψ_2^{II} are odd in θ, and $\lim_{r\to 0}\sqrt{2\pi r}\;\sigma_{12}(\nabla\boldsymbol{w}(r,0)) = 1$;
(3) for $\alpha = \mathrm{III}$, $\psi_1^{\mathrm{III}} = \psi_2^{\mathrm{III}} \equiv 0$, while ψ_3^{III} is odd in θ, and $\lim_{r\to 0}\sqrt{2\pi r}\;\sigma_{23}(\nabla\boldsymbol{w}(r,0)) = 1$.

We say that the functions $\{\psi_i^\alpha\}_{\alpha,i}$ are the angular variation of the asymptotic solution. These functions belong to $C^\infty(\mathbb{R})$, and they are 2π-antiperiodic (*i.e.*, $\psi_i^\alpha(\theta+2\pi) = -\psi_i^\alpha(\theta)$). Starting in the sequel, we will refer to the related functions $\{\Psi_{ij}^\alpha\}_{\alpha,i,j}$ which define the angular variation of the *asymptotic displacement gradient*: if $\boldsymbol{w} = r^{1/2}\psi_i^\alpha(\theta)\boldsymbol{e}_i$ is the mode α solution of (2.14), then

$$\nabla\boldsymbol{w}(\boldsymbol{x}) = r^{-1/2}\Psi_{ij}^\alpha(\theta)\boldsymbol{e}_i\otimes\boldsymbol{e}_j. \tag{2.15}$$

More explicitly, by the definition of the gradient operator in cylindrical coordinates,

$$\begin{aligned} \Psi_{i1}^\alpha(\theta) &= \frac{1}{2}\psi_i^\alpha(\theta)\cos\theta - \frac{\mathrm{d}\psi_i^\alpha(\theta)}{\mathrm{d}\theta}\sin\theta\\ \Psi_{i2}^\alpha(\theta) &= \frac{1}{2}\psi_i^\alpha(\theta)\sin\theta + \frac{\mathrm{d}\psi_i^\alpha(\theta)}{\mathrm{d}\theta}\cos\theta\\ \Psi_{i3}^\alpha(\theta) &= 0. \end{aligned} \tag{2.16}$$

Hence, the functions $\{\Psi_{ij}^\alpha\}_{\alpha,i,j}$ inherit the regularity and periodicity of $\{\psi_i\}_{\alpha,i}$. As presented in [17], these functions take the form $C_1\cos\left(\frac{\theta}{2}\right) + C_2\cos\left(\frac{3\theta}{2}\right) + C_3\cos\left(\frac{5\theta}{2}\right)$ or $C_1\sin\left(\frac{\theta}{2}\right) + C_2\sin\left(\frac{3\theta}{2}\right) + C_3\sin\left(\frac{5\theta}{2}\right)$, with the constants depending on the elastic moduli.

3. Main results

In this section, we recapitulate the problem-specific interaction integral functionals presented in [17] and the problem which defines the approximate stress intensity factors. We then state the main results of the manuscript. We conclude with a discussion of the significance of the theorems.

Before defining the problem-specific interaction integrals, we introduce some notation. For a function $v \in H^1(\mathcal{F})$, we may define its extension from the crack into the ρ-neighborhood *via* the closest point projection: $v \circ \boldsymbol{\pi}$. We abuse notation by writing both with the symbol v. For the extension we have

$$v(\boldsymbol{x}) = v(\boldsymbol{\pi}(\boldsymbol{x})) \quad \text{and} \quad \nabla v(\boldsymbol{x}) = v'(\boldsymbol{\pi}(\boldsymbol{x}))\nabla\boldsymbol{\pi}(\boldsymbol{x}), \tag{3.1}$$

where v' denotes differentiation of v with respect to s.

Next, given the basis

$$\begin{aligned} \boldsymbol{G}_2(s,r) &= \boldsymbol{N}(\boldsymbol{F}_c(s,r)) \\ \boldsymbol{G}_1(s,r) &= \boldsymbol{G}_2(s,r) \times \boldsymbol{g}_3(s) \\ \boldsymbol{G}_3(s,r) &= \boldsymbol{G}_1(s,r) \times \boldsymbol{G}_2(s,r), \end{aligned} \tag{3.2}$$

we define two auxiliary fields needed for the interaction integral – the *auxiliary gradient* for mode α

$$\boldsymbol{\beta}^{\mathrm{aux},\alpha}(\boldsymbol{x}) = r^{-1/2}\Psi^{\alpha}_{ij}(\theta + \zeta(s,r))\boldsymbol{G}_i(s,r) \otimes \boldsymbol{G}_j(s,r), \tag{3.3}$$

where $\{\Psi^{\alpha}_{ij}\}_{\alpha,i,j}$ are in (2.16) and the field

$$\boldsymbol{q}(\boldsymbol{x}) = q(r)\boldsymbol{G}_1(s,r), \tag{3.4}$$

where $q : (0,\infty) \to \mathbb{R}$ is any continuously differentiable cutoff function such that $q(r) = 1$ for $r \leq \rho_0 < \rho$ and $q(r) = 0$ for $r \geq \rho$. The combination $v\boldsymbol{q}$ is referred to as the *material variation*, and defines how the material domain changes when the crack front is perturbed by the extension v.

Definition 3.1. The *problem-specific interaction integral*s are the functionals $\mathcal{I}_\alpha : H^1(\mathcal{F}) \times L^2(\mathcal{N}^{\mathcal{C}}_\rho;\mathbb{R}^{3\times 3}) \to \mathbb{R}$, $\alpha = \mathrm{I},\mathrm{II},\mathrm{III}$:

$$\mathcal{I}_\alpha[v,\boldsymbol{\beta}] = \mathcal{I}^{(t)}_\alpha[v] + \mathcal{I}^{(b)}_\alpha[v] + \mathcal{I}^{(1)}_\alpha[v,\boldsymbol{\beta}] + \mathcal{I}^{(2)}_\alpha[v,\boldsymbol{\beta}] + \mathcal{I}^{(3)}_\alpha[v,\boldsymbol{\beta}], \tag{3.5}$$

where the five terms are

$$\mathcal{I}^{(t)}_\alpha[v] = \int_{\mathcal{C}^{\pm}_\rho} -v\boldsymbol{q}\cdot(\boldsymbol{\beta}^{\mathrm{aux},\alpha})^T \cdot \bar{\boldsymbol{t}}\,\mathrm{d}A \tag{3.6}$$

$$\mathcal{I}^{(b)}_\alpha[v] = \int_{\mathcal{N}^{\mathcal{C}}_\rho} -v\boldsymbol{q}\cdot(\boldsymbol{\beta}^{\mathrm{aux},\alpha})^T \cdot \bar{\boldsymbol{b}}\,\mathrm{d}V \tag{3.7}$$

$$\mathcal{I}^{(1)}_\alpha[v,\boldsymbol{\beta}] = \int_{\mathcal{N}^{\mathcal{C}}_\rho} -v\nabla\boldsymbol{q} : \overline{\boldsymbol{\Sigma}}(\boldsymbol{\beta},\boldsymbol{\beta}^{\mathrm{aux},\alpha})\,\mathrm{d}V \tag{3.8}$$

$$\mathcal{I}^{(2)}_\alpha[v,\boldsymbol{\beta}] = \int_{\mathcal{N}^{\mathcal{C}}_\rho} -v\boldsymbol{q}\cdot\overline{\boldsymbol{\lambda}}(\boldsymbol{\beta},\boldsymbol{\beta}^{\mathrm{aux},\alpha})\,\mathrm{d}V \tag{3.9}$$

$$\mathcal{I}^{(3)}_\alpha[v,\boldsymbol{\beta}] = \int_{\mathcal{N}^{\mathcal{C}}_\rho} -\boldsymbol{q}\cdot\overline{\boldsymbol{\Sigma}}(\boldsymbol{\beta},\boldsymbol{\beta}^{\mathrm{aux},\alpha})\cdot\nabla v\,\mathrm{d}V. \tag{3.10}$$

For any two tensors $\boldsymbol{\beta}^a$ and $\boldsymbol{\beta}^b$, we define

$$\overline{\boldsymbol{\Sigma}}(\boldsymbol{\beta}^a,\boldsymbol{\beta}^b) = \boldsymbol{\sigma}(\boldsymbol{\beta}^a) : \boldsymbol{\beta}^b\mathbf{1} - (\boldsymbol{\beta}^a)^T\cdot\boldsymbol{\sigma}(\boldsymbol{\beta}^b) - (\boldsymbol{\beta}^b)^T\cdot\boldsymbol{\sigma}(\boldsymbol{\beta}^a) \tag{3.11}$$

$$\overline{\boldsymbol{\lambda}}(\boldsymbol{\beta}^a,\boldsymbol{\beta}^b) = \boldsymbol{\beta}^a : \mathbb{C} : \left(\nabla\boldsymbol{\beta}^b - (\nabla\boldsymbol{\beta}^b)^T\right) - (\boldsymbol{\beta}^a)^T\cdot\mathrm{div}(\boldsymbol{\sigma}(\boldsymbol{\beta}^b))^{4}, \tag{3.12}$$

where, $\mathbf{1}$ is the second-order identity tensor, and if $\boldsymbol{T} = T_{ijk}\boldsymbol{e}_i \otimes \boldsymbol{e}_j \otimes \boldsymbol{e}_k$ is a third-order tensor with $\{\boldsymbol{e}_1, \boldsymbol{e}_2, \boldsymbol{e}_3\}$ orthonormal, we let $\boldsymbol{T}^T = T_{ikj}\boldsymbol{e}_i \otimes \boldsymbol{e}_j \otimes \boldsymbol{e}_k$.

We present the main properties of the problem-specific interaction integrals in the following theorem.

Theorem 3.2 (Properties of the problem-specific interaction integral)**.** *The following hold:*

(1) *For any $v \in H^1(\mathcal{F})$ and $\boldsymbol{\beta} \in L^2(\mathcal{N}_\rho^{\mathcal{C}}; \mathbb{R}^{3\times 3})$,*

$$\left|\mathcal{I}_\alpha^{(t)}[v]\right| \le C\|v\|_{1,\mathcal{F}} \quad \text{and} \quad \left|\mathcal{I}_\alpha^{(b)}[v]\right| \le C\|v\|_{0,\mathcal{F}}, \tag{3.13}$$

and

$$\left|\mathcal{I}_\alpha^{(i)}[v,\boldsymbol{\beta}]\right| \le \begin{cases} C\|v\|_{0,\mathcal{F}}\|\boldsymbol{\beta}\|_{0,\mathcal{N}_\rho^{\mathcal{C}}} & i = 1,2 \\ C|v|_{1,\mathcal{F}}\|\boldsymbol{\beta}\|_{0,\mathcal{N}_\rho^{\mathcal{C}}} & i = 3. \end{cases} \tag{3.14}$$

(2) *Let $\boldsymbol{u}$ be the exact solution of Problem 2.1. If Assumption 2.2 holds, then*

$$\mathcal{I}_\alpha[v, \nabla\boldsymbol{u}] = \eta_\alpha(v, K_\alpha)_{0,\mathcal{F}} =: \eta_\alpha \int_{\mathcal{F}} vK_\alpha \,\mathrm{d}s \tag{3.15}$$

for any $v \in H^1(\mathcal{F})$, where the constants η_α are given in terms of the elastic moduli:

$$\eta_{\mathrm{I}} = \eta_{\mathrm{II}} = \frac{2(1-\nu^2)}{E}, \quad \eta_{\mathrm{III}} = \frac{1}{\mu}\cdot \tag{3.16}$$

An immediate consequence of the term-wise bounds in the previous theorem is the following.

Corollary 3.3. *For any $v \in H^1(\mathcal{F})$ and $\boldsymbol{\beta}^a, \boldsymbol{\beta}^b \in L^2(\mathcal{N}_\rho^{\mathcal{C}}; \mathbb{R}^{3\times 3})$,*

$$\left|\mathcal{I}_\alpha[v,\boldsymbol{\beta}^a] - \mathcal{I}_\alpha\left[v,\boldsymbol{\beta}^b\right]\right| \le C\|v\|_{1,\mathcal{F}}\left\|\boldsymbol{\beta}^a - \boldsymbol{\beta}^b\right\|_{0,\mathcal{N}_\rho^{\mathcal{C}}}. \tag{3.17}$$

We now define the approximate stress intensity factors $\{K_\alpha^h\}_\alpha$, which belong to a finite-dimensional subspace $\mathscr{K}^{h_F} \subset H^1(\mathcal{F})$. The parameter h_F denotes the discretization level of $\mathscr{K}^{h_F}$; *e.g.*, the number of basis functions scales like $1/h_F$. We do not specify $\mathscr{K}^{h_F}$, though we request the following. There exists an integer $n \ge 2$ such that, if $K_\alpha \in H^n(\mathcal{F})$, then for C independent of K_α and h_F

$$\inf_{v\in\mathscr{K}^{h_F}} \|K_\alpha - v\|_{0,\mathcal{F}} \le Ch_F^n|K_\alpha|_{n,\mathcal{F}}, \tag{3.18}$$

which defines the order of approximation in $\mathscr{K}^{h_F}$. Meanwhile, for any $v \in \mathscr{K}^{h_F}$, we have the inverse inequality

$$\|v\|_{1,\mathcal{F}} \le Ch_F^{-1}\|v\|_{0,\mathcal{F}} \tag{3.19}$$

[4]In indicial notation, these are

$$\overline{\Sigma}_{ij}\left(\boldsymbol{\beta}^a,\boldsymbol{\beta}^b\right) = \sigma_{kl}(\boldsymbol{\beta}^a)\beta^b_{kl}\delta_{ij} - \beta^a_{ki}\sigma_{kj}\left(\boldsymbol{\beta}^b\right) - \beta^b_{ki}\sigma_{kj}(\boldsymbol{\beta}^a)$$
$$\overline{\lambda}_i\left(\boldsymbol{\beta}^a,\boldsymbol{\beta}^b\right) = \beta^a_{mn}\mathbb{C}_{mnkj}\left(\left(\nabla\boldsymbol{\beta}^b\right)_{kji} - \left(\nabla\boldsymbol{\beta}^b\right)_{kij}\right) - \beta^a_{ki}\left(\mathrm{div}\left(\boldsymbol{\sigma}\left(\boldsymbol{\beta}^b\right)\right)\right)_k,$$

where, in a Cartesian basis,

$$\left(\nabla\boldsymbol{\beta}^b\right)_{ijk} = \frac{\partial\beta^b_{ij}}{\partial x_k}$$
$$\mathrm{div}\left(\boldsymbol{\sigma}\left(\boldsymbol{\beta}^b\right)\right)_i = \sigma_{ij,j}\left(\boldsymbol{\beta}^b\right).$$

for some C independent of v and h_F, which is a consequence of the equivalence of norms in finite-dimensional spaces alongside a scaling argument.

The approximate stress intensity factors are computed for a vector field $\boldsymbol{u}^{h_B} \in H^1(\Omega^{\mathcal{C}}; \mathbb{R}^3)$ which approximates $\boldsymbol{u}$; namely, we assume that

$$\left\| \boldsymbol{u} - \boldsymbol{u}^{h_B} \right\|_{1,\Omega^{\mathcal{C}}} \leq C h_B^m, \tag{3.20}$$

where C may depend on $\boldsymbol{u}$.

With $\mathscr{K}^{h_F}$ and $\boldsymbol{u}^{h_B}$, we are ready to define the approximate stress intensity factors.

Definition 3.4. The *approximate stress intensity factor* $K_\alpha^h \in \mathscr{K}^{h_F}$ for mode $\alpha = \mathrm{I}, \mathrm{II}, \mathrm{III}$ is the unique solution of the variational problem

$$\eta_\alpha \big(v, K_\alpha^h\big)_{0,\mathcal{F}} = \mathcal{I}_\alpha \big[v, \nabla \boldsymbol{u}^{h_B}\big] \tag{3.21}$$

for any $v \in \mathscr{K}^{h_F}$.

Finally, we have the following convergence result.

Theorem 3.5. *Let $K_\alpha^h \in \mathscr{K}^{h_F}$ solve (3.21) for mode $\alpha = \mathrm{I}, \mathrm{II}, \mathrm{III}$ and any $v \in \mathscr{K}^{h_F}$. Then,*

$$\left\| K_\alpha - K_\alpha^h \right\|_{0,\mathcal{F}} \leq C_1 h_F^n + C_2 h_B^m h_F^{-1}, \tag{3.22}$$

where the constants C_1 and C_2 are independent of h_F and h_B but may depend on $\boldsymbol{u}$.

We conclude this section with the following remark, which highlights the key challenge overcome by the method proposed in [17].

Remark 3.6. From the term-wise continuity bounds in Theorem 3.2(1), we observe that $\mathcal{I}_\alpha[v, \boldsymbol{\beta}]$ is linear and continuous with respect to $v \in H^1(F)$ for any arbitrary $\boldsymbol{\beta} \in L^2(\mathcal{N}_\rho^{\mathcal{C}}; \mathbb{R}^{3\times3})$. Meanwhile, when $\boldsymbol{\beta} = \nabla \boldsymbol{u}$, identity (3.15) implies continuity of $\mathcal{I}_\alpha[v, \nabla \boldsymbol{u}]$ with respect to $v \in L^2(F)$ only. As we will discuss in the proof of Theorem 3.2(2), cancellations occur within the interaction integral when $\boldsymbol{\beta} = \nabla \boldsymbol{u}$, notably the domain integrands form an exact divergence. However, when we seek approximate stress intensity factors, $\nabla \boldsymbol{u}$ is unknown *a priori*, and we must use $\nabla \boldsymbol{u}^{h_B}$ instead of $\nabla \boldsymbol{u}$. Hence, we lose the cancellations that enable continuity in $L^2(\mathcal{F})$, and we instead settle for continuity in $H^1(\mathcal{F})$. If instead the functional $\mathcal{I}_\alpha\big[v, \nabla \boldsymbol{u}^{h_B}\big]$ were continuous with respect to $v \in L^2(\mathcal{F})$, we would no longer require the method proposed in [17].

Remark 3.7 (Periodic cracks)**.** While the analysis in this paper is particularized to cracks with closed front $\mathcal{F}$, we may also consider configurations where the geometry and loading are both S-periodic in s, which allows us to treat the problem in a single period. Examples include the semi-infinite flat crack which is growing around a periodic array of obstacles (*cf.* [15], Fig. 2), or a semi-infinite crack with a helical perturbation to the crack front (*cf.* [23], Fig. 2). For these crack configurations, the functionals defined in Definition 3.1 and the approximate SIFs in Definition 3.4 are unchanged, but the domains of integration ($\mathcal{F}$, $\mathcal{N}_\rho^{\mathcal{C}}$, and $\mathcal{C}_\rho^{\pm}$) are restricted to a single period in s.

For the subsequent analysis to hold in the periodic case, in particular Theorem 3.2(2), there are additional periodicity conditions that would need to be imposed on $\nabla \boldsymbol{u}$, the virtual extensions v and the function space $\mathscr{K}^{h_F}$, and the crack geometry. These conditions are discussed later in Remark 4.8.

4. Proof of the main results

We prove Theorems 3.2 and 3.5. To proceed in certain locations, we introduce additional results; proof of these may be found in the appendix.

4.1. Properties of the problem-specific interaction integrals

We begin by defining a tensor space which is important for the definition of the interaction integral. Close to the crack front, tensors in this space behave like the asymptotic displacement gradient (2.15), rotated into the local basis $\{\boldsymbol{g}_1, \boldsymbol{g}_2, \boldsymbol{g}_3\}$.

Definition 4.1 (Space of asymptotic displacement gradients)**.** Let

$$\mathscr{B}_T = \left\{ r^{-1/2} \sum_{\alpha=\mathrm{I}}^{\mathrm{III}} K_\alpha(s) \Psi^\alpha_{ij}(\theta) \boldsymbol{g}_i(s) \otimes \boldsymbol{g}_j(s), \quad K_\alpha \in H^1(\mathcal{F}), \quad (s, r, \theta) \in \Theta \right\}, \tag{4.1}$$

where $\{\Psi^\alpha_{ij}\}_{i,j,\alpha}$ were introduced in (2.16). For any tensor $\boldsymbol{\beta} \in \mathscr{B}_T$, $\{K_\alpha\}_\alpha$ are the stress intensity factors of $\boldsymbol{\beta}$.

We remark that $\mathscr{B}_T \subset L^2(\mathcal{N}^{\mathcal{C}}_\rho; \mathbb{R}^{3\times3})$. We next present a regularity result for the auxiliary gradient fields $\{\boldsymbol{\beta}^{\mathrm{aux},\alpha}\}_\alpha$, namely that they are the direct sum of a tensor in $\mathscr{B}_T$ and an H^1 tensor field. The proof can be found in Appendix B.

Proposition 4.2 (Regularity of $\boldsymbol{\beta}^{\mathrm{aux},\alpha}$)**.** *The tensor field* $\boldsymbol{\beta}^{\mathrm{aux},\alpha} \in \mathscr{B}_T \oplus H^1(\mathcal{N}^{\mathcal{C}}_\rho; \mathbb{R}^{3\times3})$*. Moreover,*

$$r^{1/2}\left(\nabla \boldsymbol{\beta}^{\mathrm{aux},\alpha} - (\nabla \boldsymbol{\beta}^{\mathrm{aux},\alpha})^T\right) \in L^\infty\left(\mathcal{N}^{\mathcal{C}}_\rho; \mathbb{R}^{3\times3\times3}\right)$$

and

$$r^{1/2} \mathrm{div}(\boldsymbol{\sigma}(\boldsymbol{\beta}^{\mathrm{aux},\alpha})) \in L^\infty\left(\mathcal{N}^{\mathcal{C}}_\rho; \mathbb{R}^3\right).$$

We are now ready to prove Theorem 3.2(1).

Proof of Theorem 3.2(1). For the traction term, the Sobolev Embedding theorem on manifolds (*cf.* [2]) gives $\bar{\boldsymbol{t}} \in H^{1/2}(\mathcal{C}^\pm_\rho; \mathbb{R}^3) \hookrightarrow L^4(\mathcal{C}^\pm_\rho; \mathbb{R}^3)$. Meanwhile, $\boldsymbol{\beta}^{\mathrm{aux},\alpha} \in L^p(\mathcal{C}^\pm_\rho; \mathbb{R}^{3\times3})$ for any $p < 2$, and, in particular $p = 4/3$. Because $\boldsymbol{q} \in L^\infty(\mathcal{N}_\rho; \mathbb{R}^3)$, by Hölder's inequality, $\boldsymbol{q} \cdot (\boldsymbol{\beta}^{\mathrm{aux},\alpha})^T \cdot \bar{\boldsymbol{t}} \in L^1(\mathcal{C}^\pm_\rho)$. Lastly, because $v \in H^1(\mathcal{F}) \hookrightarrow C^0(\mathcal{F}) \hookrightarrow L^\infty(\mathcal{F})$, it follows that

$$\left| -\int_{\mathcal{C}^\pm_\rho} v \boldsymbol{q} \cdot (\boldsymbol{\beta}^{\mathrm{aux},\alpha})^T \cdot \bar{\boldsymbol{t}} \,\mathrm{d}A \right| \le \|v\|_{0,\infty,\mathcal{F}} \int_{\mathcal{C}^\pm_\rho} \left| \boldsymbol{q} \cdot (\boldsymbol{\beta}^{\mathrm{aux},\alpha})^T \cdot \bar{\boldsymbol{t}} \right| \mathrm{d}A = C\|v\|_{0,\infty,\mathcal{F}} \le C\|v\|_{1,\mathcal{F}}.$$

Analysis of the remaining terms (3.7)–(3.10) follows a common set of steps. First, we show that the terms may be expressed as

$$\mathcal{I}^{(b)}_\alpha[v] = \int_{\mathcal{N}^{\mathcal{C}}_\rho} r^{-1/2} \tilde{v} \boldsymbol{\Phi}^{(b)} \cdot \bar{\boldsymbol{b}} \,\mathrm{d}V \quad \text{and} \quad \mathcal{I}^{(i)}_\alpha[v, \boldsymbol{\beta}] = \int_{\mathcal{N}^{\mathcal{C}}_\rho} r^{-1/2} \tilde{v} \boldsymbol{\Phi}^{(i)} : \boldsymbol{\beta} \,\mathrm{d}V,$$

where $|\boldsymbol{\Phi}^{(b,1,2,3)}| \in L^\infty(\mathcal{N}^{\mathcal{C}}_\rho)$ and $\tilde{v} = v'$ for $\mathcal{I}^{(3)}_\alpha[v, \boldsymbol{\beta}]$, while $\tilde{v} = v$ for the other terms. Then, accounting for the radial dependence of the Jacobian (2.8), a simple calculation shows

$$\left|\mathcal{I}^{(b)}_\alpha[v]\right| = \left| \int_{\mathcal{N}^{\mathcal{C}}_\rho} r^{-1/2} \tilde{v} \boldsymbol{\Phi}^{(b)} \cdot \bar{\boldsymbol{b}} \,\mathrm{d}V \right| \le C\left(\boldsymbol{\Phi}^{(b)}\right) \|\tilde{v}\|_{0,\mathcal{F}} \left\|\bar{\boldsymbol{b}}\right\|_{0,\mathcal{N}^{\mathcal{C}}_\rho}$$

with a similar result for the terms $\mathcal{I}^{(1,2,3)}_\alpha[v, \boldsymbol{\beta}]$ in which $\bar{\boldsymbol{b}}$ is replaced by $\boldsymbol{\beta}$.

For the body force term (3.7),

$$\boldsymbol{\Phi}^{(b)} = -\boldsymbol{q} \cdot \left(r^{1/2} \boldsymbol{\beta}^{\mathrm{aux},\alpha}\right)^T = -q \Psi^\alpha_{i1}(\theta + \zeta(s, r)) \boldsymbol{G}_i(s, r).$$

For $\mathcal{I}_\alpha^{(1)}[v,\boldsymbol{\beta}]$, we remark that $\overline{\boldsymbol{\Sigma}}(\cdot,\cdot)$ is bilinear with respect to its arguments, meaning there exists a sixth order tensor $\overline{\boldsymbol{S}}$ for which

$$\overline{\Sigma}_{ij}\big(\boldsymbol{\beta}^a,\boldsymbol{\beta}^b\big) = \overline{S}_{ijklmn}\beta^a_{kl}\beta^b_{mn},$$

where the components $\overline{S}_{ijklmn}$ depend on the elastic moduli. Hence,

$$-v(\nabla\boldsymbol{q})_{ij}\overline{\Sigma}_{ij}(\boldsymbol{\beta},\boldsymbol{\beta}^{\text{aux},\alpha}) = -v(\nabla\boldsymbol{q})_{ij}\overline{S}_{ijklmn}\beta_{kl}\beta^{\text{aux},\alpha}_{mn}.$$

Thus, we define the components of $\boldsymbol{\Phi}^{(1)}$:

$$\Phi^{(1)}_{kl} = -(\nabla\boldsymbol{q})_{ij}\overline{S}_{ijklmn}r^{1/2}\beta^{\text{aux},\alpha}_{mn}.$$

For $\mathcal{I}_\alpha^{(3)}[v,\boldsymbol{\beta}]$, a similar argument gives the components of $\boldsymbol{\Phi}^{(3)}$:

$$\Phi^{(3)}_{kl} = -q_i(\nabla\boldsymbol{\pi})_j\overline{S}_{ijklmn}r^{1/2}\beta^{\text{aux},\alpha}_{mn}.$$

Finally, for $\mathcal{I}_\alpha^{(2)}[v,\boldsymbol{\beta}]$, we use (3.12), pulling out $\boldsymbol{\beta}$:

$$-v\boldsymbol{q}\cdot\overline{\boldsymbol{\lambda}}(\boldsymbol{\beta},\boldsymbol{\beta}^{\text{aux},\alpha}) = -vq_i[\mathbb{C}_{mnkj}((\nabla\boldsymbol{\beta}^{\text{aux},\alpha})_{kji} - (\nabla\boldsymbol{\beta}^{\text{aux},\alpha})_{kij}) - (\operatorname{div}(\boldsymbol{\sigma}(\boldsymbol{\beta}^{\text{aux},\alpha})))_m\delta_{ni}]\boldsymbol{\beta}_{mn}.$$

Applying Proposition 4.2, the components of $\boldsymbol{\Phi}^{(2)}$ are

$$\Phi^{(2)}_{mn} = -q_i\Big[\mathbb{C}_{mnkj}r^{1/2}((\nabla\boldsymbol{\beta}^{\text{aux},\alpha})_{kji} - (\nabla\boldsymbol{\beta}^{\text{aux},\alpha})_{kij}) - r^{1/2}(\operatorname{div}(\boldsymbol{\sigma}(\boldsymbol{\beta}^{\text{aux},\alpha})))_m\delta_{ni}\Big].$$

□

We next turn our attention to Theorem 3.2(2), and we divide the proof into two steps. First, we derive the general interaction integral functional $\hat{\mathcal{I}} : H^1(\mathcal{F}) \times (\mathscr{B}_T \oplus H^1(\mathcal{N}_\rho^{\mathcal{C}};\mathbb{R}^{3\times 3}))^2 \times C^1(\overline{\mathcal{N}_\rho};\mathbb{R}^3) \to \mathbb{R}$:

$$\hat{\mathcal{I}}\big[v,\boldsymbol{\beta}^a,\boldsymbol{\beta}^b,\boldsymbol{q}^c\big] = \int_{\mathcal{C}_\rho^\pm} v\boldsymbol{q}^c\cdot\overline{\boldsymbol{\Sigma}}\big(\boldsymbol{\beta}^a,\boldsymbol{\beta}^b\big)\cdot\boldsymbol{n}\,\mathrm{d}A - \int_{\mathcal{N}_\rho^{\mathcal{C}}}\operatorname{div}\big(v\boldsymbol{q}^c\cdot\overline{\boldsymbol{\Sigma}}\big(\boldsymbol{\beta}^a,\boldsymbol{\beta}^b\big)\big)\,\mathrm{d}V. \tag{4.2}$$

Along the way, we prove the following lemma.

Lemma 4.3. *Let $v \in H^1(\mathcal{F})$, $\boldsymbol{\beta}^{a,b} = \boldsymbol{\beta}^{a,b}_T + \boldsymbol{\beta}^{a,b}_S \in \mathscr{B}_T \oplus H^1(\mathcal{N}_\rho^{\mathcal{C}};\mathbb{R}^{3\times 3})$ with stress intensity factors $\{K^a_\alpha\}_\alpha$ and $\{K^b_\alpha\}_\alpha$, respectively. Let $\boldsymbol{q}^c \in C^1(\overline{\mathcal{N}_\rho};\mathbb{R}^3)$ be such that $\boldsymbol{q}^c \equiv \boldsymbol{0}$ on $\partial\mathcal{N}_\rho$ and $\boldsymbol{q}^c|_{\mathcal{F}} = \boldsymbol{g}_1$. Then,*

$$\hat{\mathcal{I}}\big[v,\boldsymbol{\beta}^a,\boldsymbol{\beta}^b,\boldsymbol{q}^c\big] = \int_{\mathcal{F}} v\sum_{\alpha=\text{I}}^{\text{III}}\eta_\alpha K^a_\alpha K^b_\alpha\,\mathrm{d}s. \tag{4.3}$$

Second, equipped with the previous lemma, we show that

$$\mathcal{I}_\alpha[v,\nabla\boldsymbol{u}] = \hat{\mathcal{I}}[v,\nabla\boldsymbol{u},\boldsymbol{\beta}^{\text{aux},\alpha},\boldsymbol{q}],$$

where $\boldsymbol{q}$ is defined in (3.4).

We now turn to the proof of Lemma 4.3, which begins from the following identity (proof omitted):

Proposition 4.4. *Let $\boldsymbol{\beta}^a_T,\boldsymbol{\beta}^b_T \in \mathscr{B}_T$. Then, for any $s \in [0,S]$, if $\mathcal{D}_R(s)$ is the orthogonal section of the neighborhood $\mathcal{N}_R$ at s, and if $\boldsymbol{n}$ is the outward normal to $\mathcal{D}_R(s)$,*

$$\lim_{R\to 0}\int_{\partial\mathcal{D}_R(s)}\boldsymbol{g}_1(s)\cdot\overline{\boldsymbol{\Sigma}}(\boldsymbol{\beta}^a_T,\boldsymbol{\beta}^b_T)\cdot\boldsymbol{n}\,\mathrm{d}S = \sum_{\alpha=\text{I}}^{\text{III}}\eta_\alpha K^a_\alpha(s)K^b_\alpha(s). \tag{4.4}$$

A similar identity is given by Gosz and Moran [16], and may be verified through direct calculation using the exact expressions for $\{\Psi^{\alpha}_{ij}\}_{\alpha,i,j}$. Equation (4.4) amounts to an orthogonality result for the three modes of $\{\Psi^{\alpha}_{ij}\}_{\alpha,i,j}$.

The goal of our proof of Lemma 4.3 is to transform the left-hand-side of (4.4) to the right-hand-side of (4.2). We break this down into a number of steps. First, we use the integral over $\partial\mathcal{D}_R(s)$ to obtain a test for virtual crack extensions by integrating over $\partial\mathcal{N}_R$.

Proposition 4.5. *Under the assumptions of Lemma 4.3,*

$$\lim_{R\to 0}\int_{\partial\mathcal{N}_R} v\boldsymbol{q}^c\cdot\overline{\boldsymbol{\Sigma}}(\boldsymbol{\beta}^a_T,\boldsymbol{\beta}^b_T)\cdot\boldsymbol{n}\,\mathrm{d}A=\int_{\mathcal{F}} v\sum_{\alpha=\mathrm{I}}^{\mathrm{III}}\eta_\alpha K^a_\alpha K^b_\alpha\,\mathrm{d}s, \tag{4.5}$$

where v is extended to $\overline{\mathcal{N}_\rho}$ via the closest-point projection, cf. (3.1).

Proof. Let h be the stretch factor defined in (2.9). Because $\boldsymbol{\beta}^{a,b}_T\in\mathscr{B}_T$ (and hence $\left|\overline{\boldsymbol{\Sigma}}(\boldsymbol{\beta}^a_T,\boldsymbol{\beta}^b_T)\right|\leq C(K^a_\alpha,K^b_\alpha)R^{-1}$), while $|v\boldsymbol{q}^c h|\in L^\infty(\mathcal{N}_\rho)$, we have

$$\begin{aligned}\int_{\partial\mathcal{D}_R(s)} v\boldsymbol{q}\cdot\overline{\boldsymbol{\Sigma}}\big(\boldsymbol{\beta}^a_T,\boldsymbol{\beta}^b_T\big)\cdot\boldsymbol{n}\,h\mathrm{d}S &\leq \|v\boldsymbol{q}^c h\|_{0,\infty,\mathcal{N}_\rho}\int_{\mathcal{D}_R(s)}\big|\overline{\boldsymbol{\Sigma}}\big(\boldsymbol{\beta}^a_T,\boldsymbol{\beta}^b_T\big)\big|\,\mathrm{d}S\\ &\leq \|v\boldsymbol{q}^c h\|_{0,\infty,\mathcal{N}_\rho}2\pi C\big(K^a_\alpha,K^b_\alpha\big)<\infty.\end{aligned} \tag{4.6}$$

Here, the R^{-1} of $\overline{\boldsymbol{\Sigma}}(\boldsymbol{\beta}^a_T,\boldsymbol{\beta}^b_T)$ has been exactly canceled by the length element $\mathrm{d}S=R\,\mathrm{d}\theta$. It thus follows that we may modify (4.4) to get that

$$\lim_{R\to 0}\int_{\partial\mathcal{D}_R(s)} v\boldsymbol{q}^c\cdot\overline{\boldsymbol{\Sigma}}\big(\boldsymbol{\beta}^a_T,\boldsymbol{\beta}^b_T\big)\cdot\boldsymbol{n}\,h\,\mathrm{d}S=v\sum_{\alpha=\mathrm{I}}^{\mathrm{III}}\eta_\alpha K^a_\alpha(s)K^b_\alpha(s).$$

Integrating both sides over the crack front, we have

$$\int_{\mathcal{F}}\left[\lim_{R\to 0}\int_{\partial\mathcal{D}_R(s)} v\boldsymbol{q}^c\cdot\overline{\boldsymbol{\Sigma}}\big(\boldsymbol{\beta}^a_T,\boldsymbol{\beta}^b_T\big)\cdot\boldsymbol{n}\,h\,\mathrm{d}S\right]\mathrm{d}s=\int_{\mathcal{F}} v\sum_{\alpha=\mathrm{I}}^{\mathrm{III}}\eta_\alpha K^a_\alpha K^b_\alpha\,\mathrm{d}s. \tag{4.7}$$

Because of (4.6), we may apply the Lebesgue Dominated Convergence Theorem and Fubini's Theorem to the left-hand-side of (4.7), pulling the limit outside of the integral over $\mathcal{F}$ and combining the double integrals, respectively, to yield the conclusion. □

We next enlarge the set of tensor fields to which an expression like (4.5) is applicable from $\mathscr{B}_T$ to $\mathscr{B}_T\oplus H^1(\mathcal{N}^{\mathcal{C}}_\rho;\mathbb{R}^{3\times 3})$. We require the following result for the trace of an H^1 function over the boundary of a shrinking neighborhood; its proof may be found in Appendix C.

Lemma 4.6. *Let $f\in H^1(\mathcal{N}^{\mathcal{C}}_\rho)$. Then*

$$\lim_{R\to 0}\|f\|_{0,\partial\mathcal{N}_R}=0. \tag{4.8}$$

While the result is stated for scalar-valued functions, it trivially holds for vector- and tensor-valued functions such as $\boldsymbol{\beta}_S\in H^1(\mathcal{N}^{\mathcal{C}}_\rho;\mathbb{R}^{3\times 3})$.

Proposition 4.7. *Under the assumptions of Lemma 4.3,*

$$\lim_{R\to 0}\int_{\partial\mathcal{N}_R} v\boldsymbol{q}^c\cdot\overline{\boldsymbol{\Sigma}}\big(\boldsymbol{\beta}^a,\boldsymbol{\beta}^b\big)\cdot\boldsymbol{n}\,\mathrm{d}A=\int_{\mathcal{F}} v\sum_{\alpha=\mathrm{I}}^{\mathrm{III}}\eta_\alpha K^a_\alpha K^b_\alpha\,\mathrm{d}s. \tag{4.9}$$

Proof. Via bilinearity of $\overline{\mathbf{\Sigma}}(\cdot,\cdot)$ (and hence, of the left-hand-side of (4.9)) and the result of Proposition 4.5, it suffices to show that

$$\lim_{R\to 0}\int_{\partial\mathcal{N}_R} v\boldsymbol{q}^c\cdot\overline{\mathbf{\Sigma}}(\boldsymbol{\beta}^a_{\mathrm{I}},\boldsymbol{\beta}^b_J)\cdot\boldsymbol{n}\,\mathrm{d}A=0,\quad \text{for IJ}=\mathrm{TS},\mathrm{ST},\mathrm{SS}. \tag{4.10}$$

Let us consider the term with IJ $=$ TS. Fix $0<R<\rho$. Then

$$\left|\int_{\partial\mathcal{N}_R} v\boldsymbol{q}^c\cdot\overline{\mathbf{\Sigma}}\big(\boldsymbol{\beta}^a_T,\boldsymbol{\beta}^b_S\big)\cdot\boldsymbol{n}\,\mathrm{d}A\right|\le\|v\boldsymbol{q}^c\|_{0,\infty,\mathcal{N}_\rho}\int_{\partial\mathcal{N}_R}\big|\overline{\mathbf{\Sigma}}\big(\boldsymbol{\beta}^a_T,\boldsymbol{\beta}^b_S\big)\big|\,\mathrm{d}A\le C\|\boldsymbol{\beta}^a_T\|_{0,\partial\mathcal{N}_R}\big\|\boldsymbol{\beta}^b_S\big\|_{0,\partial\mathcal{N}_R}.$$

For the first inequality, we used the fact that $|v\boldsymbol{q}^c|\in L^\infty(\mathcal{N}_\rho)$. For the second inequality, as in the proof of Theorem 3.2(1), there exists a constant C such that $|\overline{\mathbf{\Sigma}}(\boldsymbol{\beta}^a_T,\boldsymbol{\beta}^b_S)|\le C|\boldsymbol{\beta}^a_T||\boldsymbol{\beta}^b_S|$, which we lumped with the term outside of the integral. Using the exact form of $\boldsymbol{\beta}^a_T$, we know that $\|\boldsymbol{\beta}^a_T\|_{0,\partial\mathcal{N}_R}\le C$, where the constant depends only on $\{K^a_\alpha\}_\alpha$ and is independent of R. Taking the limit as $R\to 0$, we get

$$\left|\lim_{R\to 0}\int_{\partial\mathcal{N}_R} v\boldsymbol{q}^c\cdot\overline{\mathbf{\Sigma}}\big(\boldsymbol{\beta}^a_T,\boldsymbol{\beta}^b_S\big)\cdot\boldsymbol{n}\,\mathrm{d}A\right|\le C\lim_{R\to 0}\big\|\boldsymbol{\beta}^b_S\big\|_{0,\partial\mathcal{N}_R}.$$

The TS case of (4.10) follows from Lemma 4.6. Analysis of the ST and SS terms is handled similarly. □

We are now ready to complete the proof of Lemma 4.3

Proof of Lemma 4.3. For notational convenience in this proof, we write

$$\boldsymbol{P}=v\boldsymbol{q}^c\cdot\overline{\mathbf{\Sigma}}\big(\boldsymbol{\beta}^a,\boldsymbol{\beta}^b\big).$$

Fix $0<R<\rho$. We introduce the following domain: $\mathcal{N}_\rho\setminus\overline{(\mathcal{N}_R\cup\mathcal{C})}$. This is a cut, hollow neighborhood of $\mathcal{F}$ with four boundary surfaces: the outer wall $\partial\mathcal{N}_\rho$, the inner wall $\partial\mathcal{N}_R$, and the positive and negative sides of the crack $(\mathcal{C}\cap(\mathcal{N}_\rho\setminus\mathcal{N}_R))^\pm$. In this domain, we may apply the divergence theorem

$$\int_{\mathcal{N}_\rho\setminus\overline{(\mathcal{N}_R\cup\mathcal{C})}}\mathrm{div}(\boldsymbol{P})\,\mathrm{d}V=\int_{(\mathcal{C}\cap(\mathcal{N}_\rho\setminus\mathcal{N}_R))^\pm}\boldsymbol{P}\cdot\boldsymbol{n}\,\mathrm{d}A+\int_{\partial\mathcal{N}_\rho}\boldsymbol{P}\cdot\boldsymbol{n}\,\mathrm{d}A+\int_{\partial\mathcal{N}_R}\boldsymbol{P}\cdot\boldsymbol{n}\,\mathrm{d}A. \tag{4.11}$$

Note that $\boldsymbol{n}$ is the *outward* normal to the domain $\mathcal{N}_\rho\setminus\overline{(\mathcal{N}_R\cup\mathcal{C})}$; for the last term in the previous equation, this direction is opposite to that used in the previous propositions. By assumption, $\boldsymbol{q}^c\equiv 0$ on $\partial\mathcal{N}_\rho$; hence, the second surface integral vanishes.

Now, let $R\to 0$. By Proposition 4.7, and carefully noting the direction of $\boldsymbol{n}$ on $\mathcal{N}_R$,

$$\int_{\mathcal{N}^{\mathcal{C}}_\rho}\mathrm{div}(\boldsymbol{P})\,\mathrm{d}V=\int_{\mathcal{C}^\pm_\rho}\boldsymbol{P}\cdot\boldsymbol{n}\,\mathrm{d}A-\int_{\mathcal{F}} v\sum_{\alpha=\mathrm{I}}^{\mathrm{III}}\eta_\alpha K^a_\alpha K^b_\alpha\,\mathrm{d}s.$$

Rearranging the previous equation gives (4.2) and the desired conclusion. □

We now prove Theorem 3.2(2).

Proof of Theorem 3.2(2). Let $\boldsymbol{\beta}^a=\nabla\boldsymbol{u}$ (the gradient of the solution of Problem 2.1) and let $\boldsymbol{\beta}^b=\boldsymbol{\beta}^{\mathrm{aux},\alpha}$. Proposition 4.2 states that $\boldsymbol{\beta}^{\mathrm{aux},\alpha}\in\mathscr{B}_T\oplus H^1(\mathcal{N}^{\mathcal{C}}_\rho;\mathbb{R}^{3\times 3})$, and from Assumption 2.2 it is possible to show that $\nabla\boldsymbol{u}\in\mathscr{B}_T\oplus H^1(\mathcal{N}^{\mathcal{C}}_\rho;\mathbb{R}^{3\times 3})$. Further, it is straightforward to show that $\boldsymbol{q}$ from (3.4) belongs to $C^1(\overline{\mathcal{N}_\rho};\mathbb{R}^3)$, is identically zero on $\partial\mathcal{N}_\rho$, and its restriction to the crack front is $\boldsymbol{g}_1$. Hence, by Lemma 4.3, we have

$$\hat{\mathcal{I}}[v,\nabla\boldsymbol{u},\boldsymbol{\beta}^{\mathrm{aux},\alpha},\boldsymbol{q}]=\eta_\alpha\int_{\mathcal{F}} vK_\alpha\,\mathrm{d}s.$$

It remains to show that $\mathcal{I}_\alpha[v, \nabla \boldsymbol{u}] = \hat{\mathcal{I}}[v, \nabla \boldsymbol{u}, \boldsymbol{\beta}^{\mathrm{aux},\alpha}, \boldsymbol{q}]$. For the surface integral in (4.2), we have $\boldsymbol{n} = \pm \boldsymbol{G}_2(s, r)$. By construction, $\boldsymbol{q} \perp \boldsymbol{n}$, while $\theta + \zeta(s, r) = \pm\pi$ and hence $\boldsymbol{\sigma}(\boldsymbol{\beta}^{\mathrm{aux},\alpha}) \cdot \boldsymbol{n} = \boldsymbol{0}$. Meanwhile, by Problem 2.1, $\boldsymbol{\sigma}(\nabla \boldsymbol{u}) \cdot \boldsymbol{n} = \bar{\boldsymbol{t}}$. Thus,

$$
\begin{aligned}
v\boldsymbol{q} \cdot \overline{\boldsymbol{\Sigma}}(\nabla \boldsymbol{u}, \boldsymbol{\beta}^{\mathrm{aux},\alpha}) \cdot \boldsymbol{n} &= v\Big[\boldsymbol{q} \cdot \boldsymbol{n} - \boldsymbol{q} \cdot (\nabla \boldsymbol{u})^T \cdot \boldsymbol{\sigma}(\boldsymbol{\beta}^{\mathrm{aux},\alpha}) \cdot \boldsymbol{n} - \boldsymbol{q} \cdot (\boldsymbol{\beta}^{\mathrm{aux},\alpha})^T \cdot \boldsymbol{\sigma}(\nabla \boldsymbol{u}) \cdot \boldsymbol{n}\Big] \\
&= -v\boldsymbol{q} \cdot (\boldsymbol{\beta}^{\mathrm{aux},\alpha})^T \cdot \bar{\boldsymbol{t}},
\end{aligned}
$$

and we recover the integrand of term (3.6). Next, let us expand the divergence in the volumetric integral of (4.2):

$$
\begin{aligned}
\operatorname{div}\big(v\boldsymbol{q} \cdot \overline{\boldsymbol{\Sigma}}(\nabla \boldsymbol{u}, \boldsymbol{\beta}^{\mathrm{aux},\alpha})\big) &= v\nabla \boldsymbol{q} : \overline{\boldsymbol{\Sigma}}(\nabla \boldsymbol{u}, \boldsymbol{\beta}^{\mathrm{aux},\alpha}) + v\boldsymbol{q} \cdot \operatorname{div}\big(\overline{\boldsymbol{\Sigma}}(\nabla \boldsymbol{u}, \boldsymbol{\beta}^{\mathrm{aux},\alpha})\big) \\
&\quad + \boldsymbol{q} \cdot \overline{\boldsymbol{\Sigma}}(\nabla \boldsymbol{u}, \boldsymbol{\beta}^{\mathrm{aux},\alpha}) \cdot \nabla v.
\end{aligned}
$$

We immediately recognize the first and third terms as the integrands of (3.8) and (3.10), respectively. Lastly, for the second term, we compute the divergence of $\overline{\boldsymbol{\Sigma}}(\nabla \boldsymbol{u}, \boldsymbol{\beta}^{\mathrm{aux},\alpha})$, apply the compatibility of $\nabla \boldsymbol{u}$, and equate $-\operatorname{div}(\boldsymbol{\sigma}(\nabla \boldsymbol{u}))$ with $\bar{\boldsymbol{b}}$ to yield

$$
\begin{aligned}
v\boldsymbol{q} \cdot \operatorname{div}\big(\overline{\boldsymbol{\Sigma}}(\nabla \boldsymbol{u}, \boldsymbol{\beta}^{\mathrm{aux},\alpha})\big) &= v\boldsymbol{q} \cdot \Big\{\nabla \boldsymbol{u} : \mathbb{C} : \Big(\nabla \boldsymbol{\beta}^{\mathrm{aux},\alpha} - (\nabla \boldsymbol{\beta}^{\mathrm{aux},\alpha})^T\Big) - (\nabla \boldsymbol{u})^T \cdot \operatorname{div}(\boldsymbol{\sigma}(\boldsymbol{\beta}^{\mathrm{aux},\alpha})) \\
&\qquad + \boldsymbol{\beta}^{\mathrm{aux},\alpha} : \mathbb{C} : \big(\nabla\nabla \boldsymbol{u} - (\nabla\nabla \boldsymbol{u})^T\big) - (\boldsymbol{\beta}^{\mathrm{aux},\alpha})^T \cdot \operatorname{div}(\boldsymbol{\sigma}(\nabla \boldsymbol{u}))\Big\} \\
&= v\boldsymbol{q} \cdot \overline{\boldsymbol{\lambda}}(\nabla \boldsymbol{u}, \boldsymbol{\beta}^{\mathrm{aux},\alpha}) + v\boldsymbol{q} \cdot (\boldsymbol{\beta}^{\mathrm{aux},\alpha})^T \cdot \bar{\boldsymbol{b}}.
\end{aligned}
$$

These are the integrands of (3.9) and (3.7), respectively, and we reach the conclusion. □

Remark 4.8 (Periodic cracks, continued)**.** We continue the discussion from Remark 3.7 for periodic cracks, in which we only integrate around a finite portion of the crack front. For such configurations, the conclusion of Lemma 4.3 is unchanged under the following assumptions which are natural in the periodic setting. We assume that the following are S-periodic in s: the virtual extensions v, the components in the $\{\boldsymbol{g}_i \otimes \boldsymbol{g}_j\}_{ij}$ basis of the tensor fields $\boldsymbol{\beta}^a$ and $\boldsymbol{\beta}^b$ (*i.e.*, for a tensor field $\boldsymbol{\beta}$, $\boldsymbol{g}_i(0)\cdot\boldsymbol{\beta}(0, r, \theta)\cdot\boldsymbol{g}_j(0) = \boldsymbol{g}_i(S)\cdot\boldsymbol{\beta}(S, r, \theta)\cdot\boldsymbol{g}_j(S)$), the components of $\boldsymbol{q}^c$ in the $\{\boldsymbol{g}_i\}_i$ basis (*i.e.*, $\boldsymbol{q}^c(0, r, \theta) \cdot \boldsymbol{g}_i(0) = \boldsymbol{q}^c(S, r, \theta) \cdot \boldsymbol{g}_i(S)$), and the inclination angle $\zeta(0, r) = \zeta(S, r)$.

When we apply the divergence theorem in (4.11), we must consider integration over the end caps of $\mathcal{N}_\rho^{\mathcal{C}}$ at $s = 0$ and $s = S$, which we term $\mathcal{D}_\rho^{\mathcal{C}}(0)$ and $\mathcal{D}_\rho^{\mathcal{C}}(S)$, respectively. By the periodicity assumption on ζ, we have that the limits of integration of (r, θ) on $\mathcal{D}_\rho^{\mathcal{C}}(0)$ and $\mathcal{D}_\rho^{\mathcal{C}}(S)$ are identical. Meanwhile, the assumed periodicity of v, $\boldsymbol{\beta}^a$, $\boldsymbol{\beta}^b$, and $\boldsymbol{q}^c$ cause

$$
\boldsymbol{P}(0, r, \theta) \cdot \boldsymbol{g}_i(0) = \boldsymbol{P}(S, r, \theta) \cdot \boldsymbol{g}_i(S)
$$

to hold for any (r, θ). The outward normals to $\mathcal{D}_\rho^{\mathcal{C}}(0)$ and $\mathcal{D}_\rho^{\mathcal{C}}(S)$ are $-\boldsymbol{g}_3(0)$ and $\boldsymbol{g}_3(S)$, respectively, and hence the two surface integrals precisely cancel, which leaves the conclusion of Lemma 4.3 unchanged.

To apply this result to Theorem 3.2(2), we need the above assumptions to hold on $\nabla \boldsymbol{u}$, $\boldsymbol{\beta}^{\mathrm{aux},\alpha}$, and $\boldsymbol{q}$ from (3.4). By the definitions of $\boldsymbol{\beta}^{\mathrm{aux},\alpha}$, and $\boldsymbol{q}$ in (3.3) and (3.4), respectively, the first and second assumptions are satisfied if

$$
\boldsymbol{G}_i(0, r) \cdot \boldsymbol{g}_j(0) = \boldsymbol{G}_i(S, r) \cdot \boldsymbol{g}_j(S)
$$

holds for any r and for any $i, j = 1, 2, 3$.

As an example, these conditions allow us to consider cracks on a torus with N-fold azimuthal symmetry by integrating over only $1/N$ of the tubular neighborhood.

Remark 4.9. In Assumption 2.2, we assumed that the stress intensity factors of $\boldsymbol{u}$ belonged to $H^2(\mathcal{F})$. Consequently, it was possible to show that $\nabla \boldsymbol{u} \in \mathscr{B}_T \oplus H^1(\mathcal{N}_\rho^{\mathcal{C}}; \mathbb{R}^{3\times 3})$. However, the space $\mathscr{B}_T$ only requires stress intensity factors belonging to $H^1(\mathcal{F})$. It is possible to relax the restrictions on the input tensors, *i.e.*, enlarge the space $\mathscr{B}_T \oplus H^1(\mathcal{N}_\rho^{\mathcal{C}}; \mathbb{R}^{3\times 3})$. For clarity, we opted not to do so in this paper. Nonetheless, a possible set of sufficient conditions for the enlarged space are as follows. First, to ensure $\operatorname{div}\big(v\boldsymbol{q}\cdot\overline{\boldsymbol{\Sigma}}(\boldsymbol{\beta}^a,\boldsymbol{\beta}^b)\big)$ is integrable on $\mathcal{N}_\rho^{\mathcal{C}}$ (thereby making valid (4.2)), we require tensors $\boldsymbol{\beta}^a$ and $\boldsymbol{\beta}^b$ such that $\nabla\boldsymbol{\beta}^{a,b}-(\nabla\boldsymbol{\beta}^{a,b})^T$ and $\operatorname{div}(\boldsymbol{\sigma}(\boldsymbol{\beta}^{a,b}))$ are both square integrable on $\mathcal{N}_\rho^{\mathcal{C}}$. Second, so that they do not contribute to the final value of the general interaction integral, the parts of $\boldsymbol{\beta}^a$ and $\boldsymbol{\beta}^b$ not belonging to $\mathscr{B}_T$ must satisfy (4.8). If the stress intensity factors of $\boldsymbol{u}$ belong only to $H^1(\mathcal{F})$, the first condition is still satisfied by $\nabla\boldsymbol{u}$ through symmetry of second distributional derivatives and because $\boldsymbol{u}$ solves Problem 2.1. *Via* direct calculation, the second condition is also satisfied by the part of $\nabla\boldsymbol{u}$ not belonging to $\mathscr{B}_T\oplus H^1(\mathcal{N}_\rho^{\mathcal{C}};\mathbb{R}^{3\times 3})$ (which possesses $r^{1/2}$-dependency around $\mathcal{F}$).

4.2. Convergence of the approximate stress intensity factors

We conclude this section with a proof of Theorem 3.5.

Proof of Theorem 3.5. Let $P^{h_F}K_\alpha\in\mathscr{K}^{h_F}$ be the L^2-projection of K_α into $\mathscr{K}^{h_F}$, *i.e.*,

$$\big(v,P^{h_F}K_\alpha\big)_{0,\mathcal{F}}=(v,K_\alpha)_{0,\mathcal{F}}$$

for any $v\in\mathscr{K}^{h_F}$. Then

$$\big\|K_\alpha-K_\alpha^h\big\|_{0,\mathcal{F}}\le\big\|K_\alpha-P^{h_F}K_\alpha\big\|_{0,\mathcal{F}}+\big\|P^{h_F}K_\alpha-K_\alpha^h\big\|_{0,\mathcal{F}}. \tag{4.12}$$

For the first term, by the interpolation estimate (3.18)

$$\big\|K_\alpha-P^{h_F}K_\alpha\big\|_{0,\mathcal{F}}=\inf_{v\in\mathscr{K}^{h_F}}\|K_\alpha-v\|_{0,\mathcal{F}}\le Ch_F^n|K|_{n,\mathcal{F}}. \tag{4.13}$$

For the second term, we have

$$\begin{aligned}\big\|P^{h_F}K_\alpha-K_\alpha^h\big\|_{0,\mathcal{F}}^2&=\big(P^{h_F}K_\alpha-K_\alpha^h,P^{h_F}K_\alpha-K_\alpha^h\big)_{0,\mathcal{F}}\\&=\big(P^{h_F}K_\alpha-K_\alpha^h,P^{h_F}K_\alpha\big)_{0,\mathcal{F}}-\big(P^{h_F}K_\alpha-K_\alpha^h,K_\alpha^h\big)_{0,\mathcal{F}}\\&=\big(P^{h_F}K_\alpha-K_\alpha^h,K_\alpha\big)_{0,\mathcal{F}}-\big(P^{h_F}K_\alpha-K_\alpha^h,K_\alpha^h\big)_{0,\mathcal{F}}\\&=\eta_\alpha^{-1}\mathcal{I}_\alpha\big[P^{h_F}K_\alpha-K_\alpha^h,\nabla\boldsymbol{u}\big]-\eta_\alpha^{-1}\mathcal{I}_\alpha\big[P^{h_F}K_\alpha-K_\alpha^h,\nabla\boldsymbol{u}^{h_B}\big],\end{aligned} \tag{4.14}$$

where we have used the definition of the L^2-projection, Theorem 3.2(2), and the definition of K_α^h (3.21). *Via* Corollary 3.3

$$\big\|P^{h_F}K_\alpha-K_\alpha^h\big\|_{0,\mathcal{F}}^2\le C\big\|P^{h_F}K_\alpha-K_\alpha^h\big\|_{1,\mathcal{F}}\big\|\nabla\boldsymbol{u}-\nabla\boldsymbol{u}^{h_B}\big\|_{0,\mathcal{N}_\rho^{\mathcal{C}}}.$$

Application of the inverse inequality (3.19) gives

$$\big\|P^{h_F}K_\alpha-K_\alpha^h\big\|_{0,\mathcal{F}}^2\le Ch_F^{-1}\big\|P^{h_F}K_\alpha-K_\alpha^h\big\|_{0,\mathcal{F}}\big\|\nabla\boldsymbol{u}-\nabla\boldsymbol{u}^{h_B}\big\|_{0,\mathcal{N}_\rho^{\mathcal{C}}}.$$

Dividing through by $\|P^{h_F}K_\alpha-K_\alpha^h\|_{0,\mathcal{F}}$, we get

$$\big\|P^{h_F}K_\alpha-K_\alpha^h\big\|_{0,\mathcal{F}}\le Ch_F^{-1}\big\|\nabla\boldsymbol{u}-\nabla\boldsymbol{u}^{h_B}\big\|_{0,\mathcal{N}_\rho^{\mathcal{C}}}.$$

Finally, using the convergence estimate (3.20) for $\|\boldsymbol{u}-\boldsymbol{u}^{h_B}\|_{1,\Omega^{\mathcal{C}}}$, we reach the conclusion. □

5. Numerical study of error estimates

Here, we assess the error estimate in Theorem 3.5 through a numerical example. As shown in the proof of that theorem (see (4.12), combined with (4.13) and (4.14)), the error in the stress intensity factors is bounded as

$$\left\|K_\alpha - K_\alpha^h\right\|_{0,\mathcal{F}} \le \inf_{v\in\mathscr{K}^{h_F}} \|K_\alpha - v\|_{0,F} + \frac{\left|\mathcal{I}_\alpha\left[w_\alpha^h, \nabla\boldsymbol{u}\right] - \mathcal{I}_\alpha\left[w_\alpha^h, \nabla\boldsymbol{u}^{h_B}\right]\right|}{\eta_\alpha\|w_\alpha^h\|_{0,F}} \tag{5.1}$$

where $w_\alpha^h := P^{h_F}K_\alpha - K_\alpha^h$. As stated earlier, the two terms represent interpolation errors in the crack front functions space $\mathscr{K}^{h_F}$, and consistency error in our definition of K_α^h. The functionals studied in this manuscript have no effect on the interpolation error; hence, in this section we will focus only on the consistency error, which for ease of notation we write as $\mathrm{Err}_\alpha^{(c)}$. In [17], we report the full error (3.22) for several numerical examples.

On a computer, $\mathcal{I}_\alpha[v, \nabla\boldsymbol{u}^{h_B}]$ is not computed exactly; rather, we use quadrature, which results in an operator $\mathcal{QI}_\alpha[v, \nabla\boldsymbol{u}^{h_B}]$. In [17], we proposed applying the same quadrature rules on the finite element mesh that were used for computing $\boldsymbol{u}^{h_B}$. If we take into account the quadrature-evaluated interaction integral when defining K_α^h, then the second term in the above error estimate becomes

$$\frac{\left|\mathcal{I}_\alpha\left[w_\alpha^h, \nabla\boldsymbol{u}\right] - \mathcal{QI}_\alpha\left[w_\alpha^h, \nabla\boldsymbol{u}^{h_B}\right]\right|}{\eta_\alpha\|w_\alpha^h\|_{0,F}}. \tag{5.2}$$

Since this term incorporates both inconsistency and quadrature errors, we use the shorthand $\mathrm{Err}_\alpha^{(c+q)}$. By subtracting and adding $\mathcal{I}_\alpha[w_\alpha^h, \nabla\boldsymbol{u}^{h_B}]$ in the numerator, we may partition the prior term in two, separating consistency and quadrature errors.

In the proof of Theorem 3.5, we bounded the consistency error using Corollary 3.3, the finite element error (3.20), and an inverse inequality (3.19)

$$\mathrm{Err}_\alpha^{(c)} \le C h_B^{1/2} h_F^{-1}, \tag{5.3}$$

where we have used the fact that for standard FEM (*e.g.*, [18]), the finite element error converged with order $h_B^{1/2}$. The suboptimal convergence rate results because the radial singularity in the exact elastic solution (2.11) is not well-approximated by piecewise polynomial basis functions [29]. Equivalently, the radial singularity reduces the regularity of $\boldsymbol{u}$, causing the function to belong to a space such as $H^{3/2}(\Omega^{\mathcal{C}})$, which possesses suboptimal convergence of interpolation errors [14].

Estimating the quadrature error is more challenging. Here, standard quadrature estimates like Theorem 8.5 of [13] no longer apply, as the integrands of (3.6)–(3.10) contain radial singularities from the auxiliary field $\boldsymbol{\beta}^{\mathrm{aux},\alpha}$. Furthermore, if the function space $\mathscr{K}^{h_F}$ is one with low continuity, for example the 1-D P^1 Lagrange finite element space constructed over a mesh of the crack front, then the extension of test functions v into $\mathcal{N}_\rho^{\mathcal{C}}$ also reduces the regularity of the integrand, thereby affecting quadrature convergence rates. These effects may be taken into account when constructing quadrature error estimates (*e.g.*, for a function with a radial point singularity, see [25]). Rather than perform such (long) computations, we instead assess the quadrature error alongside the consistency error through a numerical example.

5.1. Example

In this section, we explore numerically the consistency and quadrature errors using an example adapted from [17]. We consider the semi-infinite crack with straight crack front,

$$\mathcal{C} = \left\{\boldsymbol{x}\in\mathbb{R}^3 \,:\, x_1 < 0,\, x_2 = 0\right\}$$
$$\mathcal{F} = \left\{\boldsymbol{x}\in\mathbb{R}^3 \,:\, x_1 = x_2 = 0\right\},$$

subjected to 1-periodic loading along the x_3-direction. The geometry and loading for this problem are periodic in $s = x_3$, and we may verify that the conditions outlined in Remark 3.7 hold, so that our analysis is still

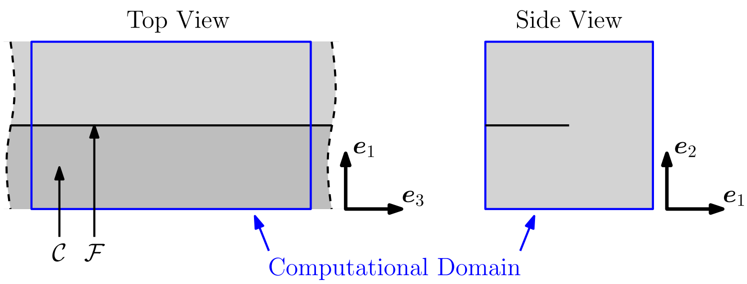

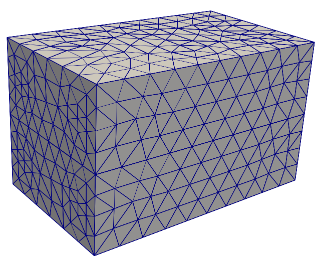

FIGURE 2. *Top*: geometry for a straight, flat crack, crack geometry. *Bottom*: perspective view showing the coarsest mesh in the family of unstructured tetrahedral meshes used for the convergence test.

valid for this problem. The crack front is straight and the crack surface is flat, hence for this geometry we have $\boldsymbol{G}_i(s,r) = \boldsymbol{g}_i(s) = \boldsymbol{e}_i$. Examples of non-planar cracks and cracks with curved fronts may be found in [17].

We construct an analytical solution with non-uniform mode II stress intensity factor by imposing appropriate tractions and body forces. The analytical displacement field around the crack front is

$$\boldsymbol{u}(\boldsymbol{x}) = K_{\mathrm{II}}(x_3) r^{1/2} \psi_i^{\mathrm{II}}(\theta) \boldsymbol{e}_i.$$

The stress intensity factor K_{II} is an even, 1-periodic function in x_3, taking value

$$K_{\mathrm{II}}(x_3) = 2 - 8(x_3 - 1/2)^2 + 16(x_3 - 1/2)^4$$

for $x_3 \in [0,1]$. For this displacement field, the crack faces are traction-free and the required body force is

$$\overline{\boldsymbol{b}}(\boldsymbol{x}) = -K_{\mathrm{II}}''(x_3)\mu r^{1/2}\big(\psi_1^{\mathrm{II}}(\theta)\boldsymbol{e}_1 + \psi_2^{\mathrm{II}}(\theta)\boldsymbol{e}_2\big) - K_{\mathrm{II}}'(x_3)(\lambda+\mu) r^{-1/2}\big(\Psi_{11}^{\mathrm{II}}(\theta) + \Psi_{22}^{\mathrm{II}}(\theta)\big)\boldsymbol{e}_3.$$

In this way, $\boldsymbol{u}$ is the solution of Problem 2.1 with body force $\overline{\boldsymbol{b}}$ and crack-face tractions $\overline{\boldsymbol{t}} \equiv \boldsymbol{0}$ on $\partial_t \Omega^{\mathcal{C}} = \mathcal{C}^{\pm}$.

5.2. Computation

We restricted our attention to the finite domain $\Omega = (-0.3, 0.3) \times (-0.3, 0.3) \times (0, 1)$. We prescribed periodic boundary conditions on the faces with $x_3 \in \{0, 1\}$, and Dirichlet boundary conditions on the faces with $|x_1| = 0.3$ and $|x_2| = 0.3$. As previously stated, the crack faces were traction free. We discretized the domain with a family of unstructured, tetrahedal meshes found through successive subdivision of each tetrahedron into eight smaller ones [24]. The problem geometry and the coarsest mesh are shown in Figure 2.

For this example, the stress intensity factors were approximated using trigonometric polynomials with maximum order $k_F \in \{5, 10, 20, 40, 80\}$. For further discussion of these spaces, see [17]. Unlike functions in the P^1 Lagrange finite element space, trigonometric polynomials are smooth, thereby eliminating a potential source of quadrature error.

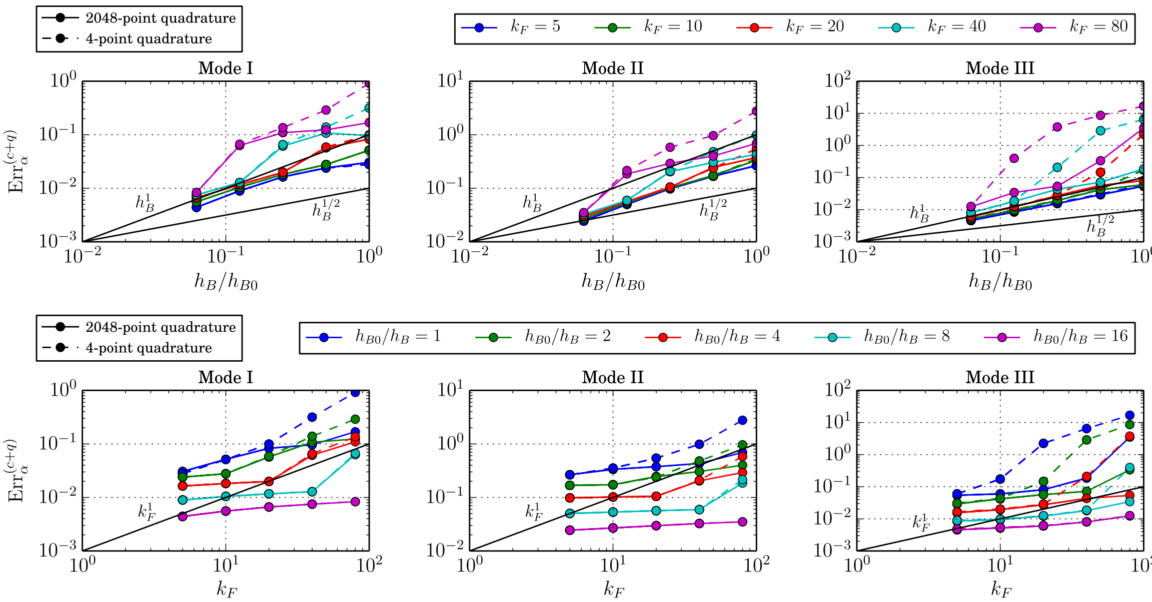

FIGURE 3. Consistency and quadrature errors (5.2) for the problem-specific interaction integral. *Top row*: variation in the errors under mesh refinement, fixing the maximum order of the spectral basis. *Bottom row*: variation in the errors with respect to the order of the spectral basis, fixing the bulk mesh refinement. Dashed lines indicate the computed errors using a four point quadrature rule in each tetrahedron, while solid lines show the errors when using 2048-point quadrature (see text). Compared with the estimate in (5.3), the errors are superconvergent with respect to bulk mesh size and more slowly growing with spectral basis order.

Numerical integration was performed using a standard, second-order quadrature rule with four points in each tetrahedron (*e.g.*, [30]). To isolate the effect of consistency error, we also used a 2048-point rule, which was found by subdividing each tetrahedron into eight smaller ones [24] three times, and applying the basic four point rule in each subdivision. With such a large number of quadrature points, we expected $\mathrm{Err}_\alpha^{(c+q)} \approx \mathrm{Err}_\alpha^{(c)}$.

5.3. Results

In Figure 3, we plot the $\mathrm{Err}_\alpha^{(c+q)}$ for the each stress intensity mode. For fixed k_F, the errors in the three terms converged with approximate order h_B, rather than the expected $h_B^{1/2}$ from (5.3).

The behavior of the error with respect to k_F was more complex. At fine values of h_B, the error grew more slowly than k_F^1. Rapid increase in the error was observed whenever $k_F(h_B/h_{B0}) > 5$. As seen in Figure 2, the coarsest mesh had $h_{B0} \approx |\mathcal{F}|/10$. Hence, the condition $k_F h_B > |\mathcal{F}|/2$ corresponded to cases where the highest wavenumber basis functions were poorly sampled on the given mesh. In practice, one would avoid such behavior, by ensuring that the highest frequencies in the crack front basis were adequately resolved on the bulk mesh.

We remark on quadrature. For each mode, quadrature errors became dominant for coarse bulk mesh size h_B and for large spectral basis order k_F. As expected in these cases, standard quadrature rules were insufficient to resolve both the radial singularities in the auxiliary fields and the rapid variation of the high wavenumber basis functions along $\mathcal{F}$. However, compared with consistency errors, quadrature errors converged more quickly with respect to h_B.

5.4. Superconvergence

We lastly comment on the appearance of superconvergence in the consistency error. As shown in Theorem 3.2(1), the problem-specific interaction integral is a continuous affine functional of the displacement field. It is well-known that continuous linear functionals applied to finite element solutions converge faster than expected from continuity (*e.g.*, [3, 4]).

The key step in classical estimates is to treat the functional (*i.e.*, $\mathcal{I}_\alpha[v, \nabla\cdot] : H^1(\Omega^{\mathcal{C}}; \mathbb{R}^3) \to \mathbb{R}$) as the data for an adjoint problem (although, in our present case, the linear elasticity operator is self-adjoint). Then the functional error may be written in terms of the dual problem's solution $\boldsymbol{w}_\alpha[v]$ and its best approximation in the finite element function space $\mathscr{V}^{h_B}$:

$$\left|\mathcal{I}_\alpha[v, \nabla \boldsymbol{u}] - \mathcal{I}_\alpha\left[v, \nabla \boldsymbol{u}^{h_B}\right]\right| \leq C\left\|\boldsymbol{u} - \boldsymbol{u}^{h_B}\right\|_{1,\Omega^{\mathcal{C}}} \inf_{\boldsymbol{w}^{h_B} \in \mathscr{V}^{h_B}} \left\|\boldsymbol{w}_\alpha[v] - \boldsymbol{w}^{h_B}\right\|_{1,\Omega^{\mathcal{C}}}.$$

Note that the previous expression assumes that $\boldsymbol{u} - \boldsymbol{u}^{h_B}$ coincide on the Dirichlet boundary. If we assume that $\boldsymbol{w}_\alpha[v]$ possesses the same regularity as $\boldsymbol{u}$, then we get the so-called "rate doubling" behavior common in the finite element literature. The errors observed in Figure 3 may be indicative of such behavior.

It is trivial to show that $\boldsymbol{w}_\alpha[v] \in H^1(\Omega^{\mathcal{C}}; \mathbb{R}^3)$; hence the best approximation error will converge [13], and the functional error will be superconvergent. However, it is unknown *a priori* whether $\boldsymbol{w}_\alpha[v]$ possesses further regularity. The answer to this open question will rely on the properties of the functional $\mathcal{I}_\alpha[v, \nabla\cdot]$ and geometric features of the problem domain $\Omega^{\mathcal{C}}$. Finally, in order to predict how changing the crack front basis $\mathscr{K}^{h_F}$ affects errors, results for the regularity of $\boldsymbol{w}_\alpha[v]$ and its best approximation must also quantify the dependence on v, a non-trivial task that requires further research.

6. Conclusion

In this work, we presented analysis of a method to approximate the stress intensity factors along the front of a three-dimensional crack. In particular, we proved that the functionals used in the method have two important properties, namely (a) that when applied to the exact displacement gradient, we recover a weighted integral of the stress intensity factors over the crack front, and (b) that the functionals are continuous. The latter property is essential for proving convergence of the method: for fixed v, the functional error is guaranteed to converge if the gradient of the finite element solution converges.

We then presented the error analysis for the numerical stress intensity factors. We showed that this error was bounded by two terms. The first term corresponded to an interpolation estimate of the stress intensity factors in the finite-dimensional function space we construct over the crack front. The second was a consistency error in the interaction integral, which we estimated *via* the continuity results of Theorem 3.2(1) and Corollary 3.3.

A numerical example provided insights beyond the error estimate of Theorem 3.5. First, quadrature errors, a practical consideration in the implementation of the method, were faster converging than the consistency error in the case where $\boldsymbol{u}^{h_B}$ was computed with standard finite elements (*e.g.*, [18]). We caution the applicability of this observation to higher-order bulk numerical schemes (*e.g.*, XFEM with singular tip enrichment or the Mapped FEM). Second, the consistency errors demonstrated superconvergent behavior, with a possible explanation being that the dual problem solution $\boldsymbol{w}_\alpha[v]$ possessed similar regularity to $\boldsymbol{u}$. Further analysis is needed to make more concrete statements on either point; however, we believe these two issues are exciting and challenging prospects for future work, as they may be crucial ingredients for ensuring rapid convergence of the numerical stress intensity factors in higher-order schemes.

Appendix A. Additional details of the near-front coordinates

Because of their use in the appendices, we introduce first a few standard preliminary relations. Notably, we present the expressions for integration over $\mathcal{N}_\rho^{\mathcal{C}}$ and $\partial\mathcal{N}_\rho$ in the tubular coordinate system, which are featured heavily in Appendix C, as well as in the proof of Theorem 3.2. We also present definitions for the gradient and divergence operator, which are used in Appendix B to prove Lemma 4.2. Additionally, for Appendix B, we prove a regularity result for the inclination angle ζ defined in (2.5).

A.1. Derivatives of basis vectors and the tubular coordinate map

Before proceeding, let us discuss the derivatives of the crack front basis vectors $\{\boldsymbol{g}_1, \boldsymbol{g}_2, \boldsymbol{g}_3\}$. Later in the appendices, we will also use the basis $\{\boldsymbol{g}_s, \boldsymbol{g}_r, \boldsymbol{g}_\theta\}$, with

$$\begin{aligned}\boldsymbol{g}_s(s) &= \boldsymbol{g}_3(s)\\ \boldsymbol{g}_r(s,\theta) &= \cos\theta\boldsymbol{g}_1(s) + \sin\theta\boldsymbol{g}_2(s)\\ \boldsymbol{g}_\theta(s,\theta) &= -\sin\theta\boldsymbol{g}_1(s) + \cos\theta\boldsymbol{g}_2(s),\end{aligned}$$

which is analogous to a cylindrical basis in the same way that $\{\boldsymbol{g}_1, \boldsymbol{g}_2, \boldsymbol{g}_3\}$ is analogous to a rectilinear basis near the crack front. To quantify derivatives of the basis vectors, we define the functions $\Gamma_{ij}(s) = \boldsymbol{g}_{i,s}(s)\cdot\boldsymbol{g}_j(s)$ for $i,j = 1,2,3$. We remark $\Gamma_{ij} = -\Gamma_{ji}$ and $\Gamma_{ii} = 0$ for $i = 1,2,3$ (no summation on i). For $\boldsymbol{g}_r$, we set

$$\boldsymbol{g}_{r,s}(s,\theta) = \Gamma_{r\theta}(s,\theta)\boldsymbol{g}_\theta(s,\theta) + \Gamma_{rs}(s,\theta)\boldsymbol{g}_s(s),$$

and the functions $\Gamma_{r\theta}$ and Γ_{rs} are related to Γ_{12}, Γ_{23} and Γ_{13}:

$$\begin{aligned}\Gamma_{r\theta}(s,\theta) &= \Gamma_{12}(s)\\ \Gamma_{rs}(s,\theta) &= \cos\theta\Gamma_{13}(s) + \sin\theta\Gamma_{23}(s) = -\boldsymbol{g}_r(s,\theta)\cdot\boldsymbol{T}_{,s}(s).\end{aligned}$$

Now, we can compute the partial derivatives of the coordinate map $\boldsymbol{X}$:

$$\begin{aligned}\frac{\partial\boldsymbol{X}}{\partial s} &= [1 + r\Gamma_{rs}(s,\theta)]\boldsymbol{g}_s(s) + r\Gamma_{12}(s)\boldsymbol{g}_\theta(s,\theta)\\ \frac{\partial\boldsymbol{X}}{\partial r} &= \boldsymbol{g}_r(s,\theta)\\ \frac{\partial\boldsymbol{X}}{\partial\theta} &= r\boldsymbol{g}_\theta(s,\theta).\end{aligned}$$

A.1.1. Regularity of the stretch factor h

The bracketed factor in the previous equation is precisely h given in (2.9). We note that $|\boldsymbol{T}_{,s}(s)| = \kappa(s)$, where κ is the curvature of the crack front at s. Because ρ is smaller than the minimum radius of curvature of $\mathcal{F}$, we must have that $0 \le r\kappa(s) \le \sup_{s\in[0,S]}\rho\kappa(s) < 1$, and hence,

$$0 < 1 - \sup_{s\in[0,S]}\rho\kappa(s) \le h(s,r,\theta) \le 1 + \sup_{s\in[0,S]}\rho\kappa(s) < 2.$$

By the strictly positive lower bound for h, we also have $h^{-1}\in L^\infty(\Theta)$. Moreover,

$$\begin{aligned}|h_{,r}(s,r,\theta)| &= |-\boldsymbol{g}_r(s,\theta)\cdot\boldsymbol{T}_{,s}(s)| \le \max_{s\in[0,S]}\kappa(s)\\ |h_{,\theta}(s,r,\theta)| &= |-r\boldsymbol{g}_\theta(s,\theta)\cdot\boldsymbol{T}_{,s}(s)| \le \max_{s\in[0,S]}\rho\kappa(s),\end{aligned}$$

while

$$|h_{,s}(s,r,\theta)| = |-r\boldsymbol{g}_r(s,\theta)\cdot\boldsymbol{T}_{,ss}(s)| < \infty.$$

Hence, $h_{,r}, h_{,\theta}, h_{,s}\in L^\infty(\Theta)$.

A.2. Integration in tubular coordinates

In the proof of Theorem 3.2 and Appendix C, we perform integration over $\mathcal{N}_\rho^{\mathcal{C}}$, $\partial\mathcal{N}_R$, and $\partial\mathcal{D}_R$ in the tubular coordinate system. Here, we derive the expressions for the relevant Jacobians.

Let $f \in L^1(\mathcal{N}_\rho^{\mathcal{C}})$. Then,

$$\int_{\mathcal{N}_\rho^{\mathcal{C}}} f \, \mathrm{d}V = \int_\Theta f \circ \boldsymbol{X} \, j \, \mathrm{d}s \, \mathrm{d}r \, \mathrm{d}\theta,$$

where

$$j = \det\left[\frac{\partial \boldsymbol{X}}{\partial s} \bigg| \frac{\partial \boldsymbol{X}}{\partial r} \bigg| \frac{\partial \boldsymbol{X}}{\partial \theta} \right] = \frac{\partial \boldsymbol{X}}{\partial s} \cdot \left(\frac{\partial \boldsymbol{X}}{\partial r} \times \frac{\partial \boldsymbol{X}}{\partial \theta} \right) = rh(s, r, \theta).$$

For integration over $\partial\mathcal{N}_R$, let $\Theta_R = \{(s, r, \theta) \in \Theta \,:\, r = R\}$, and let $\boldsymbol{X}_R$ be the restriction of $\boldsymbol{X}$ to Θ_R. Let $f \in L^1(\partial\mathcal{N}_R)$. Then

$$\int_{\partial\mathcal{N}_R} f \, \mathrm{d}A = \int_{\Theta_R} f \circ \boldsymbol{X}_R \, j_R \, \mathrm{d}s \, \mathrm{d}\theta,$$

where

$$j_R = \left| \frac{\partial \boldsymbol{X}_R}{\partial s} \times \frac{\partial \boldsymbol{X}_R}{\partial \theta} \right| = Rh(s, R, \theta).$$

Lastly, for integration over $\partial\mathcal{D}_R(s)$, we let $\boldsymbol{X}_{sR}(\theta) = \boldsymbol{X}(s, R, \theta)$. Then, if $f \in L^1(\partial\mathcal{D}_R(s))$,

$$\int_{\partial\mathcal{D}_R(s)} f \, \mathrm{d}s = \int_{-\pi-\zeta(s,R)}^{\pi-\zeta(s,R)} f \circ \boldsymbol{X}_{sR} \, j_{sR} \, \mathrm{d}\theta,$$

with

$$j_{sR} = \left| \frac{\partial \boldsymbol{X}_{sR}}{\partial \theta} \right| = R.$$

A.3. Differentiation in tubular coordinates

Because $\{\boldsymbol{g}_s, \boldsymbol{g}_r, \boldsymbol{g}_\theta\}$ is an orthonormal basis, for any differentiable function f, we wish to write

$$\nabla f = D_{\boldsymbol{g}_s} f \boldsymbol{g}_s + D_{\boldsymbol{g}_r} f \boldsymbol{g}_r + D_{\boldsymbol{g}_\theta} f \boldsymbol{g}_\theta,$$

where $D_{\boldsymbol{v}} f$ is the directional derivative of f in the direction of $\boldsymbol{v}$. Computing the directional derivatives, we can show

$$\nabla f = \frac{1}{h}\left[\frac{\partial f}{\partial s} - \Gamma_{12} \frac{\partial f}{\partial \theta} \right] \boldsymbol{g}_s + \frac{\partial f}{\partial r} \boldsymbol{g}_r + \frac{1}{r} \frac{\partial f}{\partial \theta} \boldsymbol{g}_\theta. \tag{A.1}$$

Note that this relationship holds for vector or tensor functions as well: for example, if $\boldsymbol{v}$ is a vector (or tensor) field, then

$$\nabla \boldsymbol{v} = \frac{1}{h}\left[\frac{\partial \boldsymbol{v}}{\partial s} - \Gamma_{12} \frac{\partial \boldsymbol{v}}{\partial \theta} \right] \otimes \boldsymbol{g}_s + \frac{\partial \boldsymbol{v}}{\partial r} \otimes \boldsymbol{g}_r + \frac{1}{r} \frac{\partial \boldsymbol{v}}{\partial \theta} \otimes \boldsymbol{g}_\theta.$$

A.4. Curvilinear coordinate system

In certain situations in Appendix B, it is convenient to introduce the coordinate system $\{\xi_1, \xi_2, \xi_3\}$ for the neighborhood $\mathcal{N}_\rho$ as in [16]. Here, we set

$$\Xi = \left\{ (\xi_1, \xi_2, \xi_3) \in \mathbb{R}^3 \,:\, \xi_1^2 + \xi_2^2 < \rho, \, \xi_3 \in [0, S] \right\}$$

and define the map

$$\boldsymbol{X}_\Xi(\xi_1, \xi_2, \xi_3) = \boldsymbol{F}_f(\xi_3) + \xi_1 \boldsymbol{g}_1(\xi_3) + \xi_2 \boldsymbol{g}_2(\xi_3).$$

This is a diffeomorphism between Ξ and $\mathcal{N}_\rho$. The curvilinear coordinates are related to the tubular coordinates:

$$\begin{aligned}\xi_1 &= r\cos\theta\\ \xi_2 &= r\sin\theta\\ \xi_3 &= s.\end{aligned}$$

A.4.1. Differentiation in the curvilinear coordinate system

The gradient operator in the $\{\xi_1, \xi_2, \xi_3\}$ coordinate system, expressed in the $\{\boldsymbol{g}_1, \boldsymbol{g}_2, \boldsymbol{g}_3\}$ basis, is

$$\nabla f = \frac{\partial f}{\partial \xi_1}\boldsymbol{g}_1 + \frac{\partial f}{\partial \xi_2}\boldsymbol{g}_2 + \frac{1}{h}\left[\frac{\partial f}{\partial \xi_3} + \xi_2\Gamma_{12}\frac{\partial f}{\partial \xi_1} - \xi_1\Gamma_{12}\frac{\partial f}{\partial \xi_2}\right]\boldsymbol{g}_3. \tag{A.2}$$

Later in Appendix B, when applying the above formula, we will rewrite the $\boldsymbol{g}_3$-component as

$$\frac{1}{h}\left[\frac{\partial f}{\partial \xi_3} - \Gamma_{12}\frac{\partial f}{\partial \theta}\right]$$

which makes use of the chain rule:

$$f_{,\theta} = \xi_1 f_{,2} - \xi_2 f_{,1}.$$

A.4.2. Divergence in the curvilinear coordinate system

In Appendix B, we also require an expression for the divergence of a tensor field, to which we build up starting from the divergence of a vector field. Let $\boldsymbol{v}$ be a vector field

$$\boldsymbol{v} = v_1\boldsymbol{g}_1 + v_2\boldsymbol{g}_2 + v_3\boldsymbol{g}_3.$$

Then $\mathrm{div}(\boldsymbol{v}) = \mathrm{tr}(\nabla\boldsymbol{v})$. Using the previous expression for the gradient, we may derive show

$$\mathrm{div}(\boldsymbol{v}) = v_{1,1} + v_{2,2} + \frac{1}{h}[v_{3,3} + v_1\Gamma_{13} + v_2\Gamma_{23} + \xi_2\Gamma_{12}v_{3,1} - \xi_1\Gamma_{12}v_{3,2}]. \tag{A.3}$$

Next, let $\boldsymbol{\sigma}$ be a tensor field and $\boldsymbol{a}$ is any constant vector:

$$\boldsymbol{\sigma} = \sigma_{ij}\boldsymbol{g}_i \otimes \boldsymbol{g}_j, \qquad \boldsymbol{a} = (\boldsymbol{a}\cdot\boldsymbol{g}_i)\boldsymbol{g}_i.$$

Then, $\mathrm{div}(\boldsymbol{\sigma})\cdot\boldsymbol{a} = \mathrm{div}(\boldsymbol{\sigma}^T\cdot\boldsymbol{a})$ for any constant vector $\boldsymbol{a}$. *Via* lengthy calculations, we can show

$$\begin{aligned}\mathrm{div}(\boldsymbol{\sigma}^T\cdot\boldsymbol{a}) = (\boldsymbol{a}\cdot\boldsymbol{g}_1)\Bigg[&\sigma_{11,1} + \sigma_{12,2} + \frac{1}{h}\sigma_{13,3} + \frac{1}{h}\Gamma_{21}\sigma_{23} + \frac{1}{h}\Gamma_{31}\sigma_{33}\\ &+ \frac{1}{h}\Gamma_{13}\sigma_{11} + \frac{1}{h}\Gamma_{23}\sigma_{12} + \frac{1}{h}\xi_2\Gamma_{12}\sigma_{13,1} - \frac{1}{h}\xi_1\Gamma_{12}\sigma_{13,2}\Bigg]\\ + (\boldsymbol{a}\cdot\boldsymbol{g}_2)\Bigg[&\sigma_{21,1} + \sigma_{22,2} + \frac{1}{h}\sigma_{23,3} + \frac{1}{h}\Gamma_{12}\sigma_{13} + \frac{1}{h}\Gamma_{32}\sigma_{33}\\ &+ \frac{1}{h}\Gamma_{13}\sigma_{21} + \frac{1}{h}\Gamma_{23}\sigma_{22} + \frac{1}{h}\xi_2\Gamma_{12}\sigma_{23,1} - \frac{1}{h}\xi_1\Gamma_{12}\sigma_{23,2}\Bigg]\\ + (\boldsymbol{a}\cdot\boldsymbol{g}_3)\Bigg[&\sigma_{31,1} + \sigma_{32,2} + \frac{1}{h}\sigma_{33,3} + \frac{1}{h}\Gamma_{13}\sigma_{13} + \frac{1}{h}\Gamma_{23}\sigma_{23}\\ &+ \frac{1}{h}\Gamma_{13}\sigma_{31} + \frac{1}{h}\Gamma_{23}\sigma_{32} + \frac{1}{h}\xi_2\Gamma_{12}\sigma_{33,1} - \frac{1}{h}\xi_1\Gamma_{12}\sigma_{33,2}\Bigg].\end{aligned} \tag{A.4}$$

The coefficients of $\boldsymbol{a}\cdot\boldsymbol{g}_i$ are the $\boldsymbol{g}_i$-components of $\mathrm{div}(\boldsymbol{\sigma})$. Again, when applying this expression, we will use the chain rule to rewrite

$$\frac{1}{h}\Gamma_{12}[\xi_2\sigma_{i3,1}-\xi_1\sigma_{i3,2}]=\frac{1}{h}\Gamma_{12}\sigma_{i3,\theta}.$$

A.5. Properties of the inclination angle

We recall that the inclination angle $\zeta:[0,S]\times(0,\rho)\to\mathbb{R}$ is defined in (2.5) as

$$\zeta(s,r)=\mathrm{atan2}((\boldsymbol{F}_c(s,r)-\boldsymbol{F}_f(s))\cdot\boldsymbol{g}_2(s),-(\boldsymbol{F}_c(s,r)-\boldsymbol{F}_f(s))\cdot\boldsymbol{g}_1(s)),$$

taken over the principal branch $(-\pi,\pi)$. We also recall that for any $(x,y)\in\mathbb{R}^2\setminus\{x\le 0 \text{ and } y=0\}$

$$\mathrm{atan2}(y,x)=2\tan^{-1}\left(\frac{y}{\sqrt{x^2+y^2}+x}\right)$$

and $\mathrm{atan2}\in C^\infty(\mathbb{R}^2\setminus\{x\le 0 \text{ and } y=0\})$. Because the derivatives of ζ appear in numerous places in the proofs of Appendix B, we show the following.

Proposition A.1. *The inclination angle* $\zeta\in C^1([0,S]\times[0,\rho])$.

Proof. It is straightforward to see that $\zeta\in C^\infty([0,S]\times(0,\rho))$, which results from the regularity of $\boldsymbol{F}_c$, $\boldsymbol{F}_f$, $\boldsymbol{g}_i$ and atan2. Regularity at $r=\rho$ results similarly. It remains to show regularity in the limit as $r\to 0$. Let us define

$$y(s,r):=(\boldsymbol{F}_c(s,r)-\boldsymbol{F}_f(s))\cdot\boldsymbol{g}_2(s)\quad\text{and}\quad x(s,r):=-(\boldsymbol{F}_c(s,r)-\boldsymbol{F}_f(s))\cdot\boldsymbol{g}_1(s),$$

noting that $x^2(s,r)+y^2(s,r)=r^2$. Then, we may write

$$\zeta(s,r)=2\tan^{-1}\left(\frac{y(s,r)}{r+x(s,r)}\right).$$

Given this definition of ζ, it is fairly straightforward to show that $\lim_{r\to 0}\zeta(s,r)=0$ for all s. Hence $\zeta\in C^0([0,S]\times[0,\rho])$.

Next, let us compute the derivatives of ζ as $r\to 0$. Because $r\sin\zeta=y$, we have

$$\sin\zeta+r\cos\zeta\zeta_{,r}=y_{,r}.$$

Rearranging

$$\zeta_{,r}=\frac{1}{r\cos\zeta}\left[y_{,r}(s,r)-\frac{y(s,r)}{r}\right]=\frac{1}{r\cos\zeta}\left[y_{,r}(s,r)-\frac{y(s,r)-y(s,0)}{r}\right].$$

Next, let us perform an expansion of y in the variable r. For some $0<r'<r$, we have

$$y(s,r)=y(s,0)+ry_{,r}(s,0)+\frac{1}{2}r^2y_{,rr}(s,r'),$$

while for $0<r''<r$,

$$y_{,r}(s,r)=y_{,r}(s,0)+ry_{,rr}(s,r'').$$

Noting that $y_{,r}(s,0)=0$, this yields

$$\zeta_{,r}=\frac{1}{r\cos\zeta}\left[ry_{,rr}(s,r'')-\frac{1}{2}ry_{,rr}(s,r')\right]=\frac{1}{\cos\zeta}\left[y_{,rr}(s,r'')-\frac{1}{2}y_{,rr}(s,r')\right].$$

Taking the limit as $r\to 0$ gives

$$\zeta_{,r}(s,0)=\frac{1}{2}y_{,rr}(s,0)=\frac{1}{2}\boldsymbol{F}_{c,rr}(s,0)\cdot\boldsymbol{g}_2(s),$$

which is finite. Repeating the prior procedure for the s-derivative yields

$$\zeta_{,s}(s,0) = \boldsymbol{F}_{c,sr}(s,0)\cdot\boldsymbol{g}_2(s) + |\boldsymbol{F}_{c,r}(s,0)|\Gamma_{12}(s)$$

which is also finite. Hence, we conclude that $\zeta \in C^1([0,S]\times[0,\rho])$. □

Appendix B. Properties of the auxiliary gradient fields

In this section, we prove Lemma 4.2, using the following results.

Proposition B.1. *For each* $\alpha = \mathrm{I}, \mathrm{II}, \mathrm{III}$, *let*

$$\boldsymbol{\beta}^\alpha(\boldsymbol{x}) = r^{-1/2}\Psi^\alpha_{ij}(\theta)\boldsymbol{g}_i(s)\otimes\boldsymbol{g}_j(s) \in \mathscr{B}_T. \tag{B.1}$$

Then,

$$r^{1/2}\Big(\nabla\boldsymbol{\beta}^\alpha - (\nabla\boldsymbol{\beta}^\alpha)^T\Big) \in L^\infty\big(\mathcal{N}^{\mathcal{C}}_\rho;\mathbb{R}^{3\times3\times3}\big)$$

and

$$r^{1/2}\mathrm{div}(\boldsymbol{\sigma}(\boldsymbol{\beta}^\alpha)) \in L^\infty\big(\mathcal{N}^{\mathcal{C}}_\rho;\mathbb{R}^3\big).$$

Proposition B.2. *For each* $\alpha = \mathrm{I}, \mathrm{II}, \mathrm{III}$, *let* $\boldsymbol{\beta}^\alpha_S = \boldsymbol{\beta}^{\mathrm{aux},\alpha} - \boldsymbol{\beta}^\alpha$. *Then* $\boldsymbol{\beta}^\alpha_S \in H^1(\mathcal{N}^{\mathcal{C}}_\rho;\mathbb{R}^{3\times3})$. *Moreover,* $r^{1/2}\nabla\boldsymbol{\beta}^\alpha_S \in L^\infty(\mathcal{N}^{\mathcal{C}}_\rho;\mathbb{R}^{3\times3\times3})$.

Proof of Propositions B.1 and B.2 are performed *via* direct calculation.

Proof of Proposition B.1. We first show that $r^{1/2}\big(\nabla\boldsymbol{\beta}^\alpha - (\nabla\boldsymbol{\beta}^\alpha)^T\big) \in L^\infty(\mathcal{N}^{\mathcal{C}}_\rho;\mathbb{R}^{3\times3\times3})$. By the definition of the gradient operator (A.2),

$$\begin{aligned}\nabla\boldsymbol{\beta}^\alpha = {}& \Big(r^{-1/2}\Psi^\alpha_{ij}\Big)_{,1}\boldsymbol{g}_i\otimes\boldsymbol{g}_j\otimes\boldsymbol{g}_1 + \Big(r^{-1/2}\Psi^\alpha_{ij}\Big)_{,2}\boldsymbol{g}_i\otimes\boldsymbol{g}_j\otimes\boldsymbol{g}_2\\ &+ \frac{1}{h}r^{-1/2}\Psi^\alpha_{ij}(\Gamma_{ik}\boldsymbol{g}_k\otimes\boldsymbol{g}_j + \Gamma_{jk}\boldsymbol{g}_i\otimes\boldsymbol{g}_k)\otimes\boldsymbol{g}_3 - \frac{1}{h}\Gamma_{12}r^{-1/2}\Psi^\alpha_{ij,\theta}\boldsymbol{g}_i\otimes\boldsymbol{g}_j\otimes\boldsymbol{g}_3.\end{aligned}$$

Because $(r^{-1/2}\Psi^\alpha_{ij})_{,3} = 0$ for any i,j, we can write

$$\nabla\boldsymbol{\beta}^\alpha = \Big(r^{-1/2}\Psi^\alpha_{ij}\Big)_{,k}\boldsymbol{g}_i\otimes\boldsymbol{g}_j\otimes\boldsymbol{g}_k + \frac{1}{h}r^{-1/2}\Psi^\alpha_{ij}(\Gamma_{ik}\boldsymbol{g}_k\otimes\boldsymbol{g}_j + \Gamma_{jk}\boldsymbol{g}_i\otimes\boldsymbol{g}_j)\otimes\boldsymbol{g}_3 - \frac{1}{h}\Gamma_{12}r^{-1/2}\Psi^\alpha_{ij,\theta}\boldsymbol{g}_i\otimes\boldsymbol{g}_j\otimes\boldsymbol{g}_3.$$

Denoting the first term $\boldsymbol{B}^{(1)}$,

$$\boldsymbol{B}^{(1)} - \Big(\boldsymbol{B}^{(1)}\Big)^T = \Big(r^{-1/2}\Psi^\alpha_{ij}\Big)_{,k}\boldsymbol{g}_i\otimes\boldsymbol{g}_j\otimes\boldsymbol{g}_k - \Big(r^{-1/2}\Psi^\alpha_{ik}\Big)_{,j}\boldsymbol{g}_i\otimes\boldsymbol{g}_j\otimes\boldsymbol{g}_k = 0$$

by the fact that $(r^{-1/2}\Psi^\alpha_{ij})_{,k} = (r^{-1/2}\Psi^\alpha_{ik})_{,j}$ (since these are the second derivatives of the asymptotic displacement fields, *cf.* Problem 2.3). For the second and third terms, $\Psi^\alpha_{ij}, \Psi^\alpha_{ij,\theta} \in L^\infty(\mathbb{R})$, while $\Gamma_{ij} \subset L^\infty([0,S])$ and $h^{-1} \in L^\infty(\Theta)$. Hence, there exists a constant C for which

$$\sup_{(s,r,\theta)\in\Theta}\left|\frac{1}{h}\Psi^\alpha_{ij}(\Gamma_{ik}\boldsymbol{g}_k\otimes\boldsymbol{g}_j + \Gamma_{jk}\boldsymbol{g}_i\otimes\boldsymbol{g}_j)\otimes\boldsymbol{g}_3 - \frac{1}{h}\Gamma_{12}\Psi^\alpha_{ij,\theta}\boldsymbol{g}_i\otimes\boldsymbol{g}_j\otimes\boldsymbol{g}_3\right| \le C.$$

We next show $r^{1/2}\mathrm{div}(\boldsymbol{\sigma}(\boldsymbol{\beta}^\alpha)) \in L^\infty(\mathcal{N}^{\mathcal{C}}_\rho;\mathbb{R}^3)$. For notational convenience, we write

$$\boldsymbol{\sigma}(\boldsymbol{\beta}^\alpha) = \sigma^\alpha_{ij}(\xi_1,\xi_2)\boldsymbol{g}_i(\xi_3)\otimes\boldsymbol{g}_j(\xi_3),$$

where $\sigma_{ij}^\alpha(r,\theta) = r^{-1/2}\mathbb{C}_{ijkl}\Psi_{kl}^\alpha(\theta)$. By the expression for the divergence (A.4), we have

$$\begin{aligned}\operatorname{div}(\boldsymbol{\sigma}(\boldsymbol{\beta}^\alpha)) = &\left[\sigma_{11,1}^\alpha + \sigma_{12,2}^\alpha + \frac{1}{h}\Gamma_{21}\sigma_{23}^\alpha + \frac{1}{h}\Gamma_{31}\sigma_{33}^\alpha + \frac{1}{h}\Gamma_{13}\sigma_{11}^\alpha + \frac{1}{h}\Gamma_{23}\sigma_{12}^\alpha - \frac{1}{h}\Gamma_{12}\sigma_{13,\theta}^\alpha\right]\boldsymbol{g}_1\\ &+ \left[\sigma_{21,1}^\alpha + \sigma_{22,2}^\alpha + \frac{1}{h}\Gamma_{12}\sigma_{13}^\alpha + \frac{1}{h}\Gamma_{32}\sigma_{33}^\alpha + \frac{1}{h}\Gamma_{13}\sigma_{21}^\alpha + \frac{1}{h}\Gamma_{23}\sigma_{22}^\alpha - \frac{1}{h}\Gamma_{12}\sigma_{23,\theta}^\alpha\right]\boldsymbol{g}_2\\ &+ \left[\sigma_{31,1}^\alpha + \sigma_{32,2}^\alpha + \frac{1}{h}\Gamma_{13}\sigma_{13}^\alpha + \frac{1}{h}\Gamma_{23}\sigma_{23}^\alpha + \frac{1}{h}\Gamma_{13}\sigma_{31}^\alpha + \frac{1}{h}\Gamma_{23}\sigma_{32}^\alpha - \frac{1}{h}\Gamma_{12}\sigma_{33,\theta}^\alpha\right]\boldsymbol{g}_3.\end{aligned}$$

By (2.14) and $\sigma_{ij,3}^\alpha = 0$, the first two terms in each component add up to zero. Meanwhile, the remaining terms feature no spatial derivatives of the components σ_{ij}^α, while $\sigma_{ij,\theta}^\alpha = r^{-1/2}\mathbb{C}_{ijkl}\Psi_{kl,\theta}^\alpha$, where $\mathbb{C}_{ijkl}\Psi_{kl,\theta}^\alpha \in L^\infty(\mathbb{R})$. The conclusion results from bounding each term. □

Proof of Proposition B.2. We first show $\boldsymbol{\beta}_S^\alpha \in L^2(\mathcal{N}_\rho^\mathcal{C};\mathbb{R}^{3\times 3})$. By definition,

$$\boldsymbol{\beta}_S^\alpha = r^{-1/2}\left[\Psi_{ij}^\alpha(\theta+\zeta(s,r))\boldsymbol{G}_i(s,r)\otimes\boldsymbol{G}_j(s,r) - \Psi_{ij}^\alpha(\theta)\boldsymbol{g}_i(s)\otimes\boldsymbol{g}_j(s)\right].$$

Because $\Psi_{ij}^\alpha \in L^\infty(\mathbb{R})$, there exists a constant C such that $|\boldsymbol{\beta}_S^\alpha|^2 \le Cr^{-1} \in L^1(\mathcal{N}_\rho^\mathcal{C})$.

For $\nabla\boldsymbol{\beta}_S^\alpha$, by (A.1), the gradient operator in the basis $\{\boldsymbol{g}_s, \boldsymbol{g}_r, \boldsymbol{g}_\theta\}$, it suffices to show

$$\frac{1}{h}\left[\frac{\mathrm{d}\boldsymbol{\beta}_S^\alpha}{\mathrm{d}s} - \Gamma_{12}\frac{\mathrm{d}\boldsymbol{\beta}_{S,}^\alpha}{\mathrm{d}\theta}\right], \quad \frac{\mathrm{d}\boldsymbol{\beta}_S^\alpha}{\mathrm{d}r}, \quad \frac{1}{r}\frac{\mathrm{d}\boldsymbol{\beta}_S^\alpha}{\mathrm{d}\theta} \in L^2\big(\mathcal{N}_\rho^\mathcal{C};\mathbb{R}^{3\times 3}\big).$$

Let us start with the $\boldsymbol{g}_r$-component. By direct calculation,

$$\begin{aligned}\frac{\mathrm{d}\boldsymbol{\beta}_S^\alpha}{\mathrm{d}r} = &-\frac{1}{2}r^{-3/2}\Big[\Psi_{ij}^\alpha(\theta+\zeta(s,r))\boldsymbol{G}_i(s,r)\otimes\boldsymbol{G}_j(s,r) - \Psi_{ij}^\alpha(\theta)\boldsymbol{g}_i(s)\otimes\boldsymbol{g}_j(s)\Big]\\ &+ r^{-1/2}\Big[\Psi_{ij,\theta}^\alpha(\theta+\zeta(s,r))\zeta_{,r}(s,r)\boldsymbol{G}_i(s,r)\otimes\boldsymbol{G}_j(s,r)\Big]\\ &+ r^{-1/2}\Big[\Psi_{ij}^\alpha(\theta+\zeta(s,r))(\boldsymbol{G}_{i,r}(s,r)\otimes\boldsymbol{G}_j(s,r) + \boldsymbol{G}_i(s,r)\otimes\boldsymbol{G}_{j,r}(s,r))\Big].\end{aligned}$$

For the first term, we expand inside the brackets:

$$\begin{aligned}&\Psi_{ij}^\alpha(\theta+\zeta(s,r))\boldsymbol{G}_i(s,r)\otimes\boldsymbol{G}_j(s,r) - \Psi_{ij}^\alpha(\theta)\boldsymbol{g}_i(s)\otimes\boldsymbol{g}_j(s)\\ &\quad= \left[\Psi_{ij}^\alpha(\theta+\zeta(s,r)) - \Psi_{ij}^\alpha(\theta)\right]\boldsymbol{G}_i(s,r)\otimes\boldsymbol{G}_j(s,r) + \Psi_{ij}^\alpha(\theta)[\boldsymbol{G}_i(s,r)\otimes\boldsymbol{G}_j(s,r) - \boldsymbol{g}_i(s)\otimes\boldsymbol{g}_j(s)].\end{aligned}$$

Because $\Psi_{ij}^\alpha \in C^\infty(\mathbb{R})$, $\zeta_{,r} \in L^\infty([0,S]\times[0,\rho])$ (*via* Prop. A.1),

$$\Psi_{ij}^\alpha(\theta+\zeta(s,r)) - \Psi_{ij}^\alpha(\theta) \le r\sup_{\theta\in\mathbb{R}}\big|\Psi_{ij,\theta}^\alpha(\theta)\big| \sup_{(s,r)\in[0,S]\times[0,\rho]}|\zeta_{,r}| \le Cr$$

and because $\boldsymbol{G}_i, \boldsymbol{G}_{i,r} \in C^0([0,S]\times[0,\rho];\mathbb{R}^3) \hookrightarrow L^\infty([0,S]\times[0,\rho];\mathbb{R}^3)$,

$$\boldsymbol{G}_i(s,r)\otimes\boldsymbol{G}_j(s,r) - \boldsymbol{g}_i(s)\otimes\boldsymbol{g}_j(s) \le r\sup_{(s,r)\in[0,S]\times[0,\rho]}|\boldsymbol{G}_{i,r}(s,r)\otimes\boldsymbol{G}_j(s,r) + \boldsymbol{G}_i(s,r)\otimes\boldsymbol{G}_{j,r}(s,r)| \le Cr.$$

Thus, there exists C such that $r^{1/2}|\mathrm{d}\boldsymbol{\beta}_S^\alpha/\mathrm{d}r| \le C$ for all $(s,\theta) \in \Theta_r := \{(s,r',\theta)\in\Theta : r' = r\}$.

Now let us consider the $\boldsymbol{g}_\theta$-component:

$$\frac{1}{r}\frac{\mathrm{d}\boldsymbol{\beta}_S^\alpha}{\mathrm{d}\theta} = r^{-3/2}\left[\Psi_{ij,\theta}^\alpha(\theta+\zeta(s,r))\boldsymbol{G}_i(s,r)\otimes\boldsymbol{G}_j(s,r) - \Psi_{ij,\theta}^\alpha(\theta)\boldsymbol{g}_i(s)\otimes\boldsymbol{g}_j(s)\right].$$

Using similar arguments as before, there exists C for which $r^{1/2}|r^{-1}\mathrm{d}\boldsymbol{\beta}_S^\alpha/\mathrm{d}\theta| \le C$ for all $(s,\theta) \in \Theta_r$.

Finally, for the $\boldsymbol{g}_s$-component, we remark that $\boldsymbol{G}_{i,s} \in C^0([0,S]\times[0,\rho];\mathbb{R}^3) \hookrightarrow L^\infty([0,S]\times[0,\rho];\mathbb{R}^3)$, $\zeta_{,s} \in L^\infty([0,S]\times[0,\rho])$, $\Gamma_{12} \in L^\infty([0,S])$, and $h^{-1} \in L^\infty(\Theta)$. Hence, there is a constant C such that

$$\sup_{(s,\theta)\in\Theta_r} r^{1/2}\left|\frac{1}{h}\left[\frac{\mathrm{d}\boldsymbol{\beta}_S^\alpha}{\mathrm{d}s} - \Gamma_{12}\frac{\mathrm{d}\boldsymbol{\beta}_S^\alpha}{\mathrm{d}\theta}\right]\right| \le C.$$

By the previous bounds of the $\boldsymbol{g}_r$-, $\boldsymbol{g}_\theta$-, and $\boldsymbol{g}_s$-components, we have $\nabla\boldsymbol{\beta}_S^\alpha \in L^2(\mathcal{N}_\rho^{\mathcal{C}};\mathbb{R}^{3\times3\times3})$ and $r^{1/2}\nabla\boldsymbol{\beta}_S^\alpha \in L^\infty(\mathcal{N}_\rho^{\mathcal{C}};\mathbb{R}^{3\times3\times3})$. □

Proof of Lemma 4.2. The proof follows from Propositions B.1 and B.2. Completion of the proof stems from the fact that the components of the tensor $\left(\nabla\boldsymbol{\beta}_S^\alpha - (\nabla\boldsymbol{\beta}_S^\alpha)^T\right)$ and the vector $\operatorname{div}(\boldsymbol{\sigma}(\boldsymbol{\beta}_S^\alpha))$ are linear combinations of the components of $\nabla\boldsymbol{\beta}_S^\alpha$. □

Appendix C. Trace of an H^1 function on a shrinking neighborhood

This section is devoted to the proof of Lemma 4.6. For now we consider the case where f is scalar-valued, though extension to vector- or tensor-valued functions is trivial. Our proof relies on two ingredients: the construction of a diffeomorphism between $\mathcal{N}_R^{\mathcal{C}}$ and a reference domain which is independent of R, and a suitable trace inequality posed in the reference neighborhood. For a fixed R, the combination of mapping to the reference domain, applying the trace inequality, and mapping back to the physical domain will allow us to bound the above surface integral by a positive power of R, and the result follows by letting $R \to 0$.

Letting $\hat{\Theta} = [0,S]\times(0,\rho)\times(-\pi,\pi)$, we take our reference domain as $\hat{\mathcal{N}}_\rho^{\mathcal{C}} = \hat{\boldsymbol{X}}(\hat{\Theta})$, where we distinguish between the coordinate maps $\boldsymbol{X}$ of (2.7) and $\hat{\boldsymbol{X}}$, which has identical form but is defined over $\hat{\Theta}$ instead of Θ. The map from $\hat{\mathcal{N}}_\rho^{\mathcal{C}}$ to $\mathcal{N}_R^{\mathcal{C}}$ is defined as

$$\boldsymbol{\varphi}_R = \boldsymbol{X}\circ\psi_R\circ\hat{\boldsymbol{X}}^{-1},$$

where $\psi_R : \hat{\Theta} \to \Theta$ transforms the coordinates $(\hat{s},\hat{r},\hat{\theta})$ to (s,r,θ) *via*

$$s = \hat{s}, \quad r = \frac{R}{\rho}\hat{r}, \quad \theta = \hat{\theta} - \zeta\left(\hat{s}, \frac{R}{\rho}\hat{r}\right).$$

The inverse map is given by

$$\boldsymbol{\varphi}_R^{-1} = \hat{\boldsymbol{X}}\circ\psi_R^{-1}\circ\boldsymbol{X}^{-1},$$

with ψ_R^{-1} defined *via*

$$\hat{s} = s, \quad \hat{r} = \frac{\rho}{R}r, \quad \hat{\theta} = \theta + \zeta(s,r).$$

The regularity of $\boldsymbol{X}$, $\hat{\boldsymbol{X}}$, and ψ_R guarantees that $\boldsymbol{\varphi}_R$ is a diffeomorphism between $\mathcal{N}_R^{\mathcal{C}}$ and $\hat{\mathcal{N}}_\rho^{\mathcal{C}}$.

By design of $\boldsymbol{\varphi}_R$, integrals over $\partial\mathcal{N}_R$ map to integrals over $\partial\mathcal{N}_\rho$. Meanwhile, the map $\boldsymbol{\varphi}_R$ stretches within orthogonal sections of $\mathcal{N}_R$; we next derive a trace inequality which depends only on the *radial* derivatives of the function $\hat{f} = f\circ\boldsymbol{\varphi}_R$. This result follows from a similar argument to Brenner and Scott ([6], Sect. 1.6).

Proposition C.1. *There exists a constant C depending only on $\hat{\mathcal{N}}_\rho^{\mathcal{C}}$ such that for all $\hat{f} \in H^1(\hat{\mathcal{N}}_\rho^{\mathcal{C}})$,*

$$\left\|\hat{f}\right\|_{0,\partial\mathcal{N}_\rho}^2 \le C\left(\left\|\hat{f}\right\|_{0,\hat{\mathcal{N}}_\rho^{\mathcal{C}}}^2 + \left\|\hat{f}_{,\hat{r}}\right\|_{0,\hat{\mathcal{N}}_\rho^{\mathcal{C}}}^2\right). \tag{C.1}$$

Proof. For ease of writing this proof, we will drop the "hat" from all symbols (*e.g.*, we will write f instead of $\hat{f}$).

We begin by splitting $\mathcal{N}_\rho^{\mathcal{C}}$ in two. If $\Theta^+ = \Theta\cap\{(s,r,\theta) : \theta > 0\}$ (with similar definition for Θ^-), we let $\mathcal{N}_\rho^\pm = \boldsymbol{X}(\Theta^\pm)$. In other words, we extend the crack across the ligament in the $\boldsymbol{g}_1$-direction.

We let $f^\pm$ denote the restriction of f to $\mathcal{N}_\rho^\pm$. We will prove the proposition for each half neighborhood

$$\|f^\pm\|^2_{0,S_\rho^\pm} \le C\Big(\|f^\pm\|^2_{0,\mathcal{N}_\rho^+} + \|f^\pm_{,r}\|^2_{0,\mathcal{N}_\rho^+}\Big),$$

where $S_\rho^\pm = \boldsymbol{X}(\Theta^\pm \cap \{(s,r,\theta) : r = \rho\})$. The result for the full neighborhood comes from summing over both halves. Because $\mathcal{C} \subset \partial\mathcal{N}_\rho^\pm$, each half has Lipschitz boundary. Hence, $C^1(\overline{\mathcal{N}_\rho^\pm})$ is dense in $H^1(\mathcal{N}_\rho^\pm)$ (*cf.* [1], Thm. 3.18).

We now proceed for the "positive" half neighborhood. Proof for the "negative" half is nearly identical. Let $\phi \in C^1(\overline{\mathcal{N}_\rho^+})$. Then,

$$\begin{aligned} h\rho^2\phi^2(s,\rho,\theta) &= \int_0^\rho \left(hr^2\phi^2\right)_{,r} \mathrm{d}r \\ &= \int_0^\rho 2hr\phi^2 + 2hr^2\phi\phi_{,r} + r^2\phi^2 h_{,r}\,\mathrm{d}r \\ &\le 2\max\{1,\rho\}\int_0^\rho hr\phi^2 + hr|\phi\phi_{,r}| + r\phi^2|h_{,r}|\,\mathrm{d}r \\ &\le 2\max\{1,\rho\}\max\left\{1, \frac{\sup_\Theta|h_{,r}|}{\inf_\Theta h}\right\}\int_0^\rho 2hr\phi^2 + hr|\phi\phi_{,r}|\,\mathrm{d}r, \end{aligned}$$

where the last inequality results from the properties of the stretch factor h in (2.9). We next divide through by ρ and integrate both sides in θ and s:

$$\int_0^S\int_0^\pi \phi^2\, h\rho \mathrm{d}\theta\mathrm{d}s \le \frac{4}{\rho}\max\{1,\rho\}\max\left\{1, \frac{\sup_\Theta|h_{,r}|}{\inf_\Theta h}\right\}\int_0^S\int_0^\pi\int_0^\rho \left[\phi^2 + |\phi\phi_{,r}|\right] hr\,\mathrm{d}r\,\mathrm{d}\theta\,\mathrm{d}s.$$

Lumping the constant, we may bound

$$\|\phi\|^2_{0,S_\rho^+} \le C\Big(\|\phi\|^2_{0,\mathcal{N}_\rho^+} + \|\phi\phi_{,r}\|_{0,1,\mathcal{N}_\rho^+}\Big) \le C\Big(\|\phi\|^2_{0,\mathcal{N}_\rho^+} + \|\phi_{,r}\|^2_{0,\mathcal{N}_\rho^+}\Big).$$

By density, we extend the above result to $f^+ \in H^1(\mathcal{N}_\rho^+)$. Summing the results for f^+ and f^- yields the conclusion. ☐

Equipped with the mapping $\boldsymbol{\varphi}_R$ and the above trace inequality, we are now ready to prove Lemma 4.6.

Proof of Lemma 4.6. Fix R. We map to the reference neighborhood,

$$\|f\|^2_{0,\partial\mathcal{N}_R} \le \frac{\sup_\Theta h}{\inf_{\hat\Theta}\hat h}\frac{R}{\rho}\|\hat f\|^2_{0,\partial\mathcal{N}_\rho}\,^{5}.$$

Applying Proposition C.1 to the right-hand-side yields

$$\|f\|^2_{0,\partial\mathcal{N}_R} \le CR\left(\left\|\hat f\right\|^2_{0,\hat{\mathcal{N}}_\rho^{\mathcal{C}}} + \left\|\hat f_{,\hat r}\right\|^2_{0,\hat{\mathcal{N}}_\rho^{\mathcal{C}}}\right),$$

where we lumped all the constants independent of f and R into C. We apply a change of coordinates to transform the norms on the right-hand-side back to the domain $\mathcal{N}_R^{\mathcal{C}}$:

$$\|f\|^2_{0,\partial\mathcal{N}_R} \le CR\left(\frac{1}{R^2}\|f\|^2_{0,\mathcal{N}_R^{\mathcal{C}}} + |f|^2_{1,\mathcal{N}_R^{\mathcal{C}}}\right)^{6}. \tag{C.2}$$

[5] Under $\boldsymbol{\varphi}_R$, area elements of $\partial\mathcal{N}_R$ change according to $\frac{h}{\hat h}\frac{R}{\rho}$.

[6] The Jacobian of $\boldsymbol{\varphi}_R^{-1}$ is given by $\frac{\hat h}{h}\frac{\rho^2}{R^2}$, while one may show $|\hat f_{,\hat r}|^2 \le C\frac{R^2}{\rho^2}|\nabla f|^2$.

For the second term on the right-hand-side of (C.2), we have

$$|f|^2_{1,\mathcal{N}_R^{\mathcal{C}}} \leq |f|^2_{1,\mathcal{N}_\rho^{\mathcal{C}}}. \tag{C.3}$$

For the first term on the right-hand-side of (C.2), *via* the Sobolev Embedding Theorem (*cf.* [1]) we know that $H^1(\mathcal{N}_\rho^{\mathcal{C}}) \hookrightarrow L^6(\mathcal{N}_\rho^{\mathcal{C}})$, and thus

$$\|f\|_{0,6,\mathcal{N}_\rho^{\mathcal{C}}} \leq C\|f\|_{1,\mathcal{N}_\rho^{\mathcal{C}}}.$$

As a consequence, $f^2 \in L^3(\mathcal{N}_\rho^{\mathcal{C}})$, and we may apply the Hölder Inequality:

$$\|f\|^2_{0,\mathcal{N}_R^{\mathcal{C}}} \leq \|f\|^2_{0,6,\mathcal{N}_R^{\mathcal{C}}} \left|\mathcal{N}_R^{\mathcal{C}}\right|^{2/3} \leq C\|f\|^2_{1,\mathcal{N}_\rho^{\mathcal{C}}} \left|\mathcal{N}_R^{\mathcal{C}}\right|^{2/3}. \tag{C.4}$$

Putting the bounds of (C.3) and (C.4) into (C.2), and noting that $|\mathcal{N}_R^{\mathcal{C}}| = \pi R^2 S$, we get

$$\|f\|^2_{0,\partial\mathcal{N}_R} \leq CR^{1/3}\|f\|^2_{1,\mathcal{N}_\rho^{\mathcal{C}}} + CR|f|^2_{1,\mathcal{N}_\rho^{\mathcal{C}}}. \tag{C.5}$$

Letting $R \to 0$ yields the desired conclusion. □

Acknowledgements. The authors gratefully acknowledge the support for this work through grant NSF CMMI-1662452.

References

[1] R.A. Adams and J.J.F. Fournier, Sobolev Spaces. Vol. 140 of *Pure and Applied Mathematics*. Academic Press (2003).
[2] T. Aubin, Nonlinear Analysis on Manifolds. Monge-Ampère Equations. Vol. 252 of *Grundlehren der mathematischen Wissenschaften*. Springer-Verlag, New York (1982).
[3] I. Babuška and A. Miller, The post-processing approach in the finite element method – Part 1: Calculation of displacements, stresses and other higher derivatives of the displacements. *Int. J. Numer. Methods Eng.* **20** (1984) 1085–1109.
[4] I. Babuška and A. Miller, The post-processing approach in the finite element method – Part 2: the calculation of stress intensity factors. *Int. J. Numer. Methods Eng.* **20** (1984) 1111–1129.
[5] J.R. Barber, Elasticity, 3 edition. Vol. 172 of *Solid Mechanics and Its Applications*. Springer Dordrecht (2010).
[6] S. Brenner and R. Scott, The Mathematical Theory of Finite Element Methods. Vol. 15 of *Texts in Applied Mathematics*. Springer-Verlag, New York (2008).
[7] S.K. Chan, I.S. Tuba and W.K. Wilson, On the finite element method in linear fracture mechanics. *Eng. Fract. Mech.* **2** (1970) 1–17.
[8] G.P. Cherepanov, The propagation of cracks in a continuous medium. *J. Appl. Math. Mech.* **31** (1967) 503–512.
[9] M.M. Chiaramonte, Y.X. Shen, L.M. Keer and A.J. Lew, Computing stress intensity factors for curvilinear cracks. *Int. J. Numer. Methods Eng.* **104** (2015) 260–296.
[10] M.M. Chiaramonte, Y.X. Shen and A.J. Lew, Mapped finite element methods: high-order approximations of problems on domains with cracks and corners. *Int. J. Numer. Methods Eng.* **111** (2017) 864–900.
[11] M. Costabel, M. Dauge and R. Duduchava, Asymptotics without logarithmic terms for crack problems. *Commun. Part. Differ. Equ.* **28** (2003) 869–926.
[12] M. Costabel, M. Dauge and Z. Yosibash, A quasi-dual function method for extracting edge stress intensity functions. *SIAM J. Math. Anal.* **35** (2004) 1177–1202.
[13] A. Ern and J.-L. Guermond, Theory and Practice of Finite Elements. Vol. 159 of *Applied Mathematical Sciences*. Springer-Verlag, New York (2004).
[14] M. Feistauer, On the finite element approximation of functions with noninteger derivatives. *Numer. Funct. Anal. Optim.* **10** (1989) 91–110.
[15] H. Gao and J.R. Rice, A first-order perturbation analysis of crack trapping by arrays of obstacles. *J. Appl. Mech.* **56** (1989) 828–836.
[16] M Gosz and B Moran, An interaction energy integral method for computation of mixed-mode stress intensity factors along non-planar crack fronts in three dimensions. *Eng. Fract. Mech.* **69** (2002) 299–319.
[17] B.E. Grossman-Ponemon, L.M. Keer and A.J. Lew, A method to compute mixed-mode stress intensity factors for nonplanar cracks in three dimensions. *Int. J. Numer. Methods Eng.* **121** (2020) 4292–4328.
[18] T.J.R. Hughes, The Finite Element Method: Linear Static and Dynamic Finite Element Analysis. Courier Corporation, New York (2000).
[19] J.-H. Kim and G.H. Paulino, Finite element evaluation of mixed mode stress intensity factors in functionally graded materials. *Int. J. Numer. Methods Eng.* **53** (2002) 1903–1935.

[20] A.A. Kosinski, Differential Manifolds. Vol. 138 of *Pure and Applied Mathematics*. Academic Press (1993).

[21] S.G. Krantz and H.R. Parks, The Implicit Function Theorem: History, Theory, and Applications. *Modern Birkhäuser Classics*. Birkhäuser, New York (2013).

[22] J.-B. Leblond and O. Torlai, The stress field near the front of an arbitrarily shaped crack in a three-dimensional elastic body. *J. Elasticity* **29** (1992) 97–131.

[23] J.-B. Leblond, A. Karma and V. Lazarus, Theoretical analysis of crack front instability in mode I+III. *J. Mech. Phys. Solids* **59** (2011) 1872–1887.

[24] A. Liu and B. Joe, Quality local refinement of tetrahedral meshes based on 8-subtetrahedron subdivision. *Math. Comput. Am. Math. Soc.* **65** (1996) 1183–1200.

[25] J.N. Lyness, An error functional expansion for N-dimensional quadrature with an integrand function singular at a point. *Math. Comput.* **30** (1976) 1–23.

[26] N. Moës, J. Dolbow and T. Belytschko, A finite element method for crack growth without remeshing. *Int. J. Numer. Methods Eng.* **46** (1999) 131–150.

[27] G.P. Nikishkov and S.N. Atluri, Calculation of fracture mechanics parameters for an arbitrary three-dimensional crack, by the "equivalent domain integral" method. *Int. J. Numer. Methods Eng.* **24** (1987) 1801–1821.

[28] J.R. Rice, A path independent integral and the approximate analysis of strain concentration by notches and cracks. *J. Appl. Mech.* **35** (1968) 379–386.

[29] Y.X. Shen and A. Lew, An optimally convergent discontinuous Galerkin-based extended finite element method for fracture mechanics. *Int. J. Numer. Methods Eng.* **82** (2010) 716–755.

[30] L. Shunn and F. Ham, Symmetric quadrature rules for tetrahedra based on a cubic close-packed lattice arrangement. *J. Comput. Appl. Math.* **236** (2012) 4348–4364.

[31] B.A. Szabó and I. Babuška, Finite Element Analysis. John Wiley & Sons Inc, New York (1991).

[32] B.A. Szabó and I. Babuška, Computation of the amplitude of stress singular terms for cracks and reentrant corners, in Fracture Mechanics: Nineteenth Symposium. ASTM International (1988).

[33] D.M. Tracey, Finite elements for determination of crack tip elastic stress intensity factors. *Eng. Fract. Mech.* **3** (1971) 255–265.

[34] J.F. Yau, S.S. Wang and H.T. Corten, A mixed-mode crack analysis of isotropic solids using conservation laws of elasticity. *J. Appl. Mech.* **47** (1980) 335–341.

[35] Z. Yosibash, Singularities in Elliptic Boundary Value Problems and Elasticity and Their Connection with Failure Initiation. Vol. 37 of *Interdisciplinary Applied Mathematics*. Springer-Verlag, New York (2012).

[36] Z. Yosibash, S. Shannon, M. Dauge and M. Costabel, Circular edge singularities for the laplace equation and the elasticity system in 3-D domains. *Int. J. Fract.* **168** (2011) 31–52.

[37] A.T. Zehnder, Fracture Mechanics. Vol. 62 of *Lecture Notes in Applied and Computational Mechanics*. Springer, Netherlands (2012).